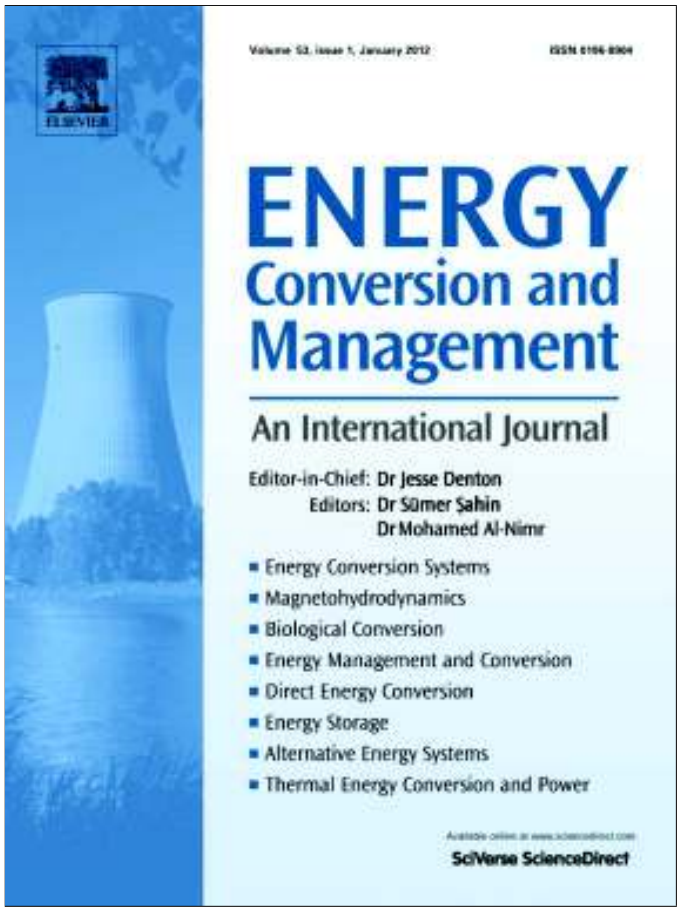

Energy Conversion and Management 73 (2013) 285–302

Contents lists available at SciVerse ScienceDirect

Energy Conversion and Management

journal homepage: www.elsevier.com/locate/enconman

Optimal integration of organic Rankine cycles with industrial processes

Brígido J. Hipólito-Valencia [a], Eusiel Rubio-Castro [b], José M. Ponce-Ortega [a,*], Medardo Serna-González [a], Fabricio Nápoles-Rivera [a], Mahmoud M. El-Halwagi [c,d]

[a] Chemical Engineering Department, Universidad Michoacana de San Nicolás de Hidalgo, Morelia, Mich. 58060, Mexico
[b] Chemical and Biological Sciences Department, Universidad Autónoma de Sinaloa, Culiacán, Sinaloa 80000, Mexico
[c] Chemical Engineering Department, Texas A&M University, College Station, TX, USA
[d] Adjunct Faculty at the Chemical and Materials Engineering Department, Faculty of Engineering, King Abdulaziz University, P.O. Box 80204, Jeddah 21589, Saudi Arabia

ARTICLE INFO

Article history:
Received 18 February 2013
Accepted 23 April 2013

Keywords:
Energy integration
Waste process heat recovery
Organic Rankine cycle
Electricity generation
Heat exchanger network
Optimization

ABSTRACT

This paper presents a procedure for simultaneously handling the problem of optimal integration of regenerative organic Rankine cycles (ORCs) with overall processes. ORCs may allow the recovery of an important fraction of the low-temperature process excess heat (i.e., waste heat from industrial processes) in the form of mechanical energy. An integrated stagewise superstructure is proposed for representing the interconnections and interactions between the HEN and ORC for fixed data of process streams. Based on the integrated superstructure, the optimization problem is formulated as a mixed integer nonlinear programming problem to simultaneously account for the capital and operating costs including the revenue from the sale of the shaft power produced by the integrated system. The application of this method is illustrated with three example problems. Results show that the proposed procedure provides significantly better results than an earlier developed method for discovering optimal integrated systems using a sequential approach, due to the fact that it accounts simultaneously for the tradeoffs between the capital and operating costs as well as the sale of the produced energy. Also, the proposed method is an improvement over the previously reported methods for solving the synthesis problem of heat exchanger networks without the option of integration with an ORC (i.e., stand-alone heat exchanger networks).

1. Introduction

Nowadays the energy savings as well as the environmental impact minimization are important concerns in the process industry. In this regard, one of the most important strategies implemented to solve this problem is the implementation of heat exchanger networks (HENs). A large number of methods has been published for the optimal synthesis of HENs over the past three decades [1–4]. Basically, these procedures are based on sequential and simultaneous approaches. Among them, the pinch analysis [5–7] is one of the most successful sequential strategies, while mathematical programming techniques [8–14] are required to implement simultaneous approaches for synthesizing HENs.

The methods based on pinch analysis for synthesizing HENs have been focused on determining targets including the minimum consumption of hot and cold utilities, the minimum number of heat-transfer units and the minimum heat transfer area (to generate the economic trade-offs between capital and operating costs ahead of design). The targets for hot and cold utilities typically can be obtained using the composite curves [15], the table algorithm [16] and direct numerical geometric-based techniques [17]. Also, to determine the minimum utility cost there are some methods that consider constant temperatures [11], not constant temperatures [18] and account for design constraints such as forbidden matches between the process streams [19]. Papoulias and Grossmann [11] formulated a transshipment model and Viswanathan and Evans [18] proposed a method based on the out-of-kilter algorithm to calculate the minimum utility cost for multiple utilities. Recently, Serna-González et al. [19] proposed an algorithm to calculate the area targets for HENs with different heat transfer coefficients and non-uniform exchanger specifications. Then, Serna-Gonzalez and Ponce-Ortega [20] developed a new method for simultaneous targeting of network area and pumping power cost. Castier [21] presented a rigorous sequential multiple utility targeting approach. Moreover, several approaches for HEN retrofitting based on sequential approaches have been reported [22–24].

Respect to the mathematical programming-based approaches, the work by Yee and Grossmann [13] represents a basic framework for the optimal synthesis of HENs. This problem is formulated as a mixed integer non-linear programming (MINLP) problem, which is based on a superstructure that is a stagewise representation where within each stage heat exchange can occur between participating

* Corresponding author. Tel./fax: +52 443 3273584.
E-mail address: jmponce@umich.mx (J.M. Ponce-Ortega).

0196-8904/$ - see front matter © 2013 Elsevier Ltd. All rights reserved.
http://dx.doi.org/10.1016/j.enconman.2013.04.036

Nomenclature

Binary variables

z_j^{cond}	binary variables for the match between the ORC condenser and cold process stream j
z^{acu}	binary variables for the match between the ORC condenser and cold utility in the ORC
z_i^{cu}	binary variables for the match between hot process stream i and cold utility in the HEN
z_i^{evap}	binary variables for the match between hot process stream i and the organic fluid in the ORC evaporator
z_j^{hu}	binary variables for the match between hot utility and cold process stream j in the HEN
$z_{i,j,k}$	binary variables for match (i, j) in stage k of the superstructure of the HEN

Greek letters

β^{cond}	exponent for area of condensers in cost equation
β^{cu}	exponent for area of coolers in cost equation
β^{hu}	exponent for area of heaters in cost equation
β^{econ}	exponent for area of regenerator in cost equation
β^{evap}	exponent for area of evaporators in cost equation
β^{exch}	exponent for area of exchangers in cost equation
β^{pump}	exponent for power of pump in cost equation
β^{turb}	exponent for power of turbine in cost equation
δ	small number
η^{econ}	efficiency parameter of the regenerator
η^{ORC}	efficiency parameter of the ORC
η^{pump}	efficiency parameter of the pump

Parameters

C^{acu}	unit cost of cold utility for ORC
C^{cu}	unit cost of cold utility
C^{hu}	unit cost of hot utility
C^{power}	unit price of power generated
C^{pump}	unit cost of pumping power
CF^{cond}	unit fixed cost for the condensers
CF^{acu}	fixed charge associated with the ORC coolers
CF^{cu}	fixed charge associated with the HEN coolers
CF^{econ}	fixed charge associated with the regenerator
CF^{evap}	fixed charge associated with the ORC evaporators
CF^{hu}	fixed charge associated with the HEN heaters
CF	fixed charge associate with the HEN exchangers
CF^{pump}	fixed charge associated with the organic fluid pump
CF^{turb}	fixed charge associated with the ORC turbine
Cp_i	specific heat capacity for hot process stream i
Cp_j	specific heat capacity for cold process stream j
CV^{acu}	variable cost coefficient for the ORC coolers
CV^{cond}	variable cost coefficient for the ORC condensers
CV^{cu}	variable cost coefficient for the HEN coolers
CV^{econ}	variable cost coefficient for the regenerator
CV^{evap}	variable cost coefficient for the ORC evaporators
CV^{hu}	variable cost coefficient for the HEN heaters
CV	variable cost coefficient for heat transfer units in the HEN
CV^{pump}	variable cost coefficient for the ORC pump
CV^{turb}	variable cost coefficient for the ORC turbine
$dt^{acu\text{-}hot}$	temperature difference at hot end of ORC condensers using cold utility
$dt^{acu\text{-}cold}$	temperature difference at cold end of ORC condensers using cold utility
$dt^{econ\text{-}hot}$	temperature difference at hot end of the ORC regenerator
$dt^{econ\text{-}cold}$	temperature difference at cold end of the ORC regenerator
F	flow rate
FCp_i	heat capacity flow rate for hot process stream i
FCp_j	heat capacity flow rate for cold process stream j
h_i	film heat transfer coefficient for hot process stream i
h^{cu}	film heat transfer coefficient for the cold utility used in the HEN
h^{hu}	film heat transfer coefficient for the hot utility used in the HEN
h_j	film heat transfer coefficient for cold process stream j
h^{evap}	film heat transfer coefficient for the organic working fluid in the evaporators of the ORC
h^{cond}	film heat transfer coefficient for the organic working fluid in the condensers of the ORC
h^{acu}	film heat transfer coefficient for the cold utility of the ORC
$h^{econ\text{-}hot}$	film heat transfer coefficient for the organic working fluid at hot side of the regenerator of the ORC
$h^{econ\text{-}cold}$	film heat transfer coefficient for the organic working fluid at cold side of the regenerator of the ORC
H_Y	annual operating time
K_F	factor used to annualize capital costs
Q_i^{max}	upper bound for heat load of hot process stream i
Q_j^{max}	upper bound for heat load of cold process stream j
$Q_{i,j}^{max}$	upper bound for the heat exchanged in the match (i,j)
T^{turb}	organic fluid outlet temperature of turbine
TIN^{cond}	organic fluid inlet temperature of the ORC condensers
TIN^{acu}	inlet temperature for the cold utility in the ORC
TIN_i	inlet temperature of hot process stream i
TIN_j	inlet temperature of cold process stream j
TIN^{evap}	organic fluid inlet temperature of the ORC evaporators
$TOUT^{cond}$	organic fluid outlet temperature of the ORC condensers
$TOUT^{acu}$	outlet temperature of the cold utility in the ORC
$TOUT_i$	outlet temperature of hot process stream i
$TOUT_j$	outlet temperature of cold process stream j
$TOUT^{evap}$	organic fluid outlet temperature of the ORC evaporators
$\Delta T^{cond\text{-}max}$	upper bound for temperature difference for condensers
$\Delta T^{acu\text{-}max}$	upper bound for temperature difference for cold utility of the ORC
$\Delta T_i^{cu\text{-}max}$	upper bound for temperature difference for cold utility
$\Delta T^{evap\text{-}max}$	upper bound for temperature difference for evaporators
$\Delta T_j^{hu\text{-}max}$	upper bound for temperature difference for hot utility
$\Delta T_{i,j}^{max}$	upper bound for temperature difference for exchangers
ΔT^{min}	minimum approach temperature difference

Scripts

cond	condensers
cu	cold utility
econ	regenerator
exch	exchangers
evap	evaporators
hu	hot utility
NOK	total number of stages
ORC	organic Rankine cycle
turb	turbine

Sets

CPS	set for cold process streams j
HPS	set for hot process streams i
i	index for hot process streams
j	index for cold process streams
k	index for stages $(1, \ldots, NOK)$ and temperature locations $(1, \ldots, NOK + 1)$
ST	set for stages in the superstructure k

Variables

Cap	capital cost
Capf	fixed capital cost
Capv	variable capital cost
Cop	operating cost
$dt_i^{\text{cu-hot}}$	temperature difference at hot end of the match between hot process stream i and the cold utility
$dt_i^{\text{cu-cold}}$	temperature difference at cold end of the match between hot process stream i and the cold utility
$dt_j^{\text{cond-hot}}$	temperature difference at hot end of the match between the organic fluid and cold process stream j (ORC condenser)
$dt_j^{\text{cond-cold}}$	temperature difference at cold end of the match between the organic fluid and cold process stream j (ORC condenser)
$dt_i^{\text{evap-hot}}$	temperature difference at hot end of the match between hot process stream i and the organic fluid (ORC evaporator)
$dt_i^{\text{evap-cold}}$	temperature difference at cold end of the match between hot process stream i and the organic fluid (ORC evaporator)
$dt_j^{\text{hu-hot}}$	temperature difference at hot end of the match between cold process stream j and the hot utility
$dt_j^{\text{hu-cold}}$	temperature difference at cold end of the match between cold process stream j and the hot utility
$dt_{i,j,k}^{\text{hot}}$	temperature difference at hot end of the match (i,j) at temperature location k
$dt_{i,j,k+1}^{\text{cold}}$	temperature difference at cold end of the match (i,j) at temperature location k
E^{pump}	power consumed by the ORC pump
E^{ORC}	power generated by the ORC
q_j^{cond}	heat exchanged between the organic fluid and cold process stream j in an ORC condenser
q_i^{cu}	cold utility requirement for hot process stream i
Q^{acu}	cold utility requirement for the ORC
q_j^{evap}	heat exchanged between cold process stream j and the organic fluid in an ORC condenser
q_j^{hu}	hot utility requirement for cold process stream j
$q_{i,j,k}$	heat exchanged between hot process stream i and cold process stream j at stage k of the HEN
Q^{total}	total heat load of the ORC condensers
Q^{econ}	heat load of the regenerator
Sprc	revenue from the sale of the electricity that is generated in the ORC
TAC	total annual cost
t_i^{ORC}	outlet temperature of hot process stream i from an ORC evaporator
$t_{i,k}$	temperature of hot process stream i at hot end of stage k
$t_{j,k}$	temperature of cold process stream j at hot end of stage k

hot and cold process streams and external utilities are placed only at the extremes of the superstructure (see Fig. 1a). This MINLP stage-based superstructure allows obtaining parallel, series and/or series–parallel arrangements of heat transfer units. The objective function consists in minimizing the total annual cost formed by operating and capital costs. To tackle several HEN problems, the network superstructure given by Yee and Grossmann [13] has been extended by several authors. For example, some flexibility aspects for designing HENs were considered by Verheyen and Zhang [25], Chen and Hung [26] and Konukman et al. [27]. The detailed heat-exchanger design and the pressure drops effects on the synthesis of HENs were included by Serna-González et al. [28], Mizutani et al. [29], Frausto-Hernández et al. [30] and Ponce-Ortega et al. [31]. For multipass heat exchanger networks, Ponce-Ortega et al. [32] developed a synthesis methodology using the stagewise network superstructure in conjunction with genetic algorithms. Other authors have shown how the retrofit problem of HENs can be formulated based on this superstructure [33,34]. Approaches to include isothermal process streams have also been reported [35–37]. Recently, Ponce-Ortega et al. [38] proposed an extension of the superstructure by Yee and Grossmann [13] to include the optimal placement of multiple utilities (see Fig. 1b), and then based on this superstructure Lopez-Maldonado et al. [39] included environmental criteria in the HEN synthesis. Additional works for energy integration using network superstructures similar to the one proposed by Yee and Grossmann [13] have been developed for the synthesis of cooling water systems [40–44] and absorption refrigeration systems [45–47].

In heat exchanger networks, process heat is recovered by exchanging it between hot process streams that have to be cooled and cold process streams that have to be heated. Since the total heat content of the hot and cold streams is usually unequal, and because of thermodynamic constraints for heat transfer (i.e., non-negative temperature differences), usually utilities are required to provide the auxiliary heating and cooling to decrease or increase the temperatures of hot and cold process streams to reach specified values. In this context, several cold utilities (i.e., cooling water, air and refrigeration at different levels) are usually used to meet the total cold utility load of processes. However, commonly an important fraction of process excess heat is rejected to cold utilities at a temperature level at which it could be recovered in the form of mechanical power. In particular, an amount of process excess heat (i.e., low temperature and intermediate sensible heat) could be reutilized as heat source for an organic Rankine cycle (ORC), where it would be converted into power with a given efficiency. The ORC is similar to the conventional steam Rankine cycle but the former cycle uses an organic fluid instead of water as working fluid for power generation. [48–58]. Organic fluids are desirable as working fluids for low temperature application due to their low boiling temperature, medium vapor pressure at moderate temperature, low specific volume, and low isentropic turbine enthalpy drop. Various authors have proposed several approaches for the selection of the organic Rankine fluids [59–66]. In general, dry and isentropic organic working fluids with positive and nearly infinitely large slopes (dT/dS), respectively, are the ones that provide better ORC performance for low temperature heat recovery [50,59–61]. To thermally improve ORCs, regeneration using an economizer (regenerator) has been included in the structure of ORC in recent works [61,62].

Recently, Desai and Bandyopadhyay [61] have proposed a sequential method based on pinch analysis for integrating ORCs with processes to generate shaft-work and, at the same time, to reduce the overall cold utility requirement. The solution is carried out in a three-step procedure. Firstly, for a given value of the minimum allowed approach temperature ($\Delta T_{\min}$), the minimum consumption of hot and cold utilities for a process are predicted using the problem table algorithm and the grand composite curve (GCC). Then, in the second step, heat absorption profiles (i.e., targeting of evaporation temperature and load) for the ORC placed entirely below the process pinch (also termed the bottoming cycle in the integrated system under consideration) are obtained using the process GCC. Once the optimum heat absorbing profile is identi-

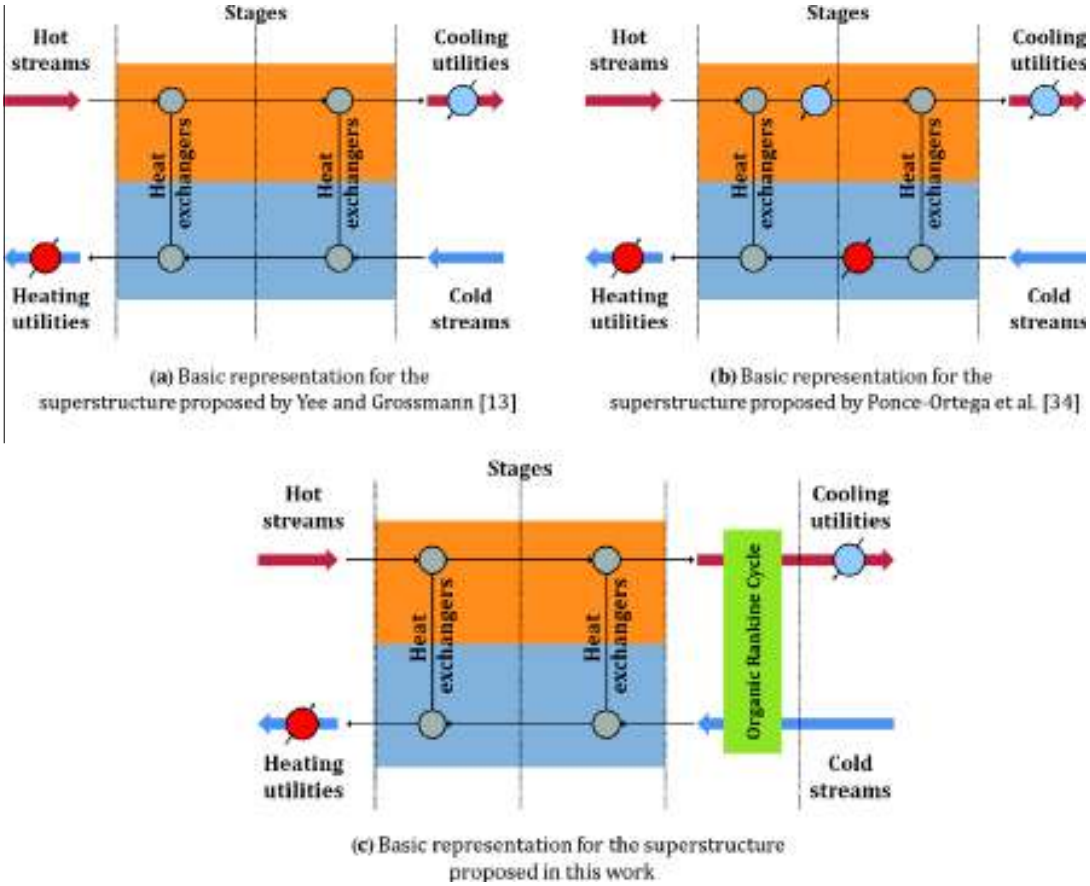

Fig. 1. Basic representations of proposed superstructures for synthesizing HEN.

fied, in the last step a feasible configuration of the heat exchanger network integrated with the ORC is developed. It should be noted that the minimum utility consumption and the maximum production of shaft-work are the objectives of this sequential method. Therefore, it generates bottoming cogeneration cycle plants that are energy efficient; however, the designs obtained will feature optimal or near optimal costs only when the cost of utilities is the dominant cost item in the system. Another important objective is to minimize the total annual cost of HENs integrated with ORCs, since the optimal design normally involves a trade-off between investment costs for equipment in the integrated system (heat transfer units, turbine and pump) and the minimum utility consumption costs. In this case, the obtained designs would be both economically attractive and energy efficient.

The problem of synthesizing HENs integrated with regenerative ORCs via simultaneous structural and parameter optimization is addressed in this paper. Based on a stagewise superstructure (see Fig. 1c) for embedding all the alternative heat integration configurations of interest, a mixed integer nonlinear programming framework is presented to determine the configuration, design parameters and operation variables of bottoming cogeneration cycle plants which minimize the total annual cost. The advantage of this approach is that it explicitly accounts for the economic trade-offs and interactions in the synthesis problem of these integrated systems.

2. Problem statement

The problem addressed in this paper can be stated as follows: Given are a set of hot process streams that have to be cooled and a set of cold process streams that have to be heated, with known inlet and outlet temperatures, and heat capacity flow rates. Given are also the data for the cold and hot utilities (inlet and outlet temperatures and unitary costs). Additional data are the correlations of capital costs for equipment in the heat exchanger network and the ORC (heat transfer units, turbine and pump), and the unit price for the electric power produced in the ORC. Also, the technical constraints associated to the performance of the ORC with regenerative working fluid heating are specified, including the type of the dry organic working fluid participating in the integrated system and its saturation temperatures in the evaporator and condenser (i.e., temperature levels) of the cycle. Then the synthesis problem consists in determining the configuration, the produced electricity, design parameters, and operation variables for the integrated HEN–ORC system that minimize the total annual cost accounting simultaneously for the cost of utilities, capital cost for equipment as well as the revenue from the sale of power produced by the ORC.

The regenerative ORC considered in this paper is represented in the temperature-entropy diagram shown in Fig. 2a and schematically represented in Fig. 2b. This cycle involves five thermodynamic processes indicated in Fig. 2a. As shown in this figure, the cycle begins at state (1) with saturated liquid. The dry organic working fluid is pumped to state (2). To improve the thermal efficiency of the ORC, a regenerator is used to allow the interchange of energy between the turbine exhaust that is in the superheated vapor region at state (5) and the compressed liquid entering the evaporator. In this process, the liquid is heated from state (2) to state (7). An external low-grade heat source is then used in the evaporator where the dry organic working fluid vaporizes at con-

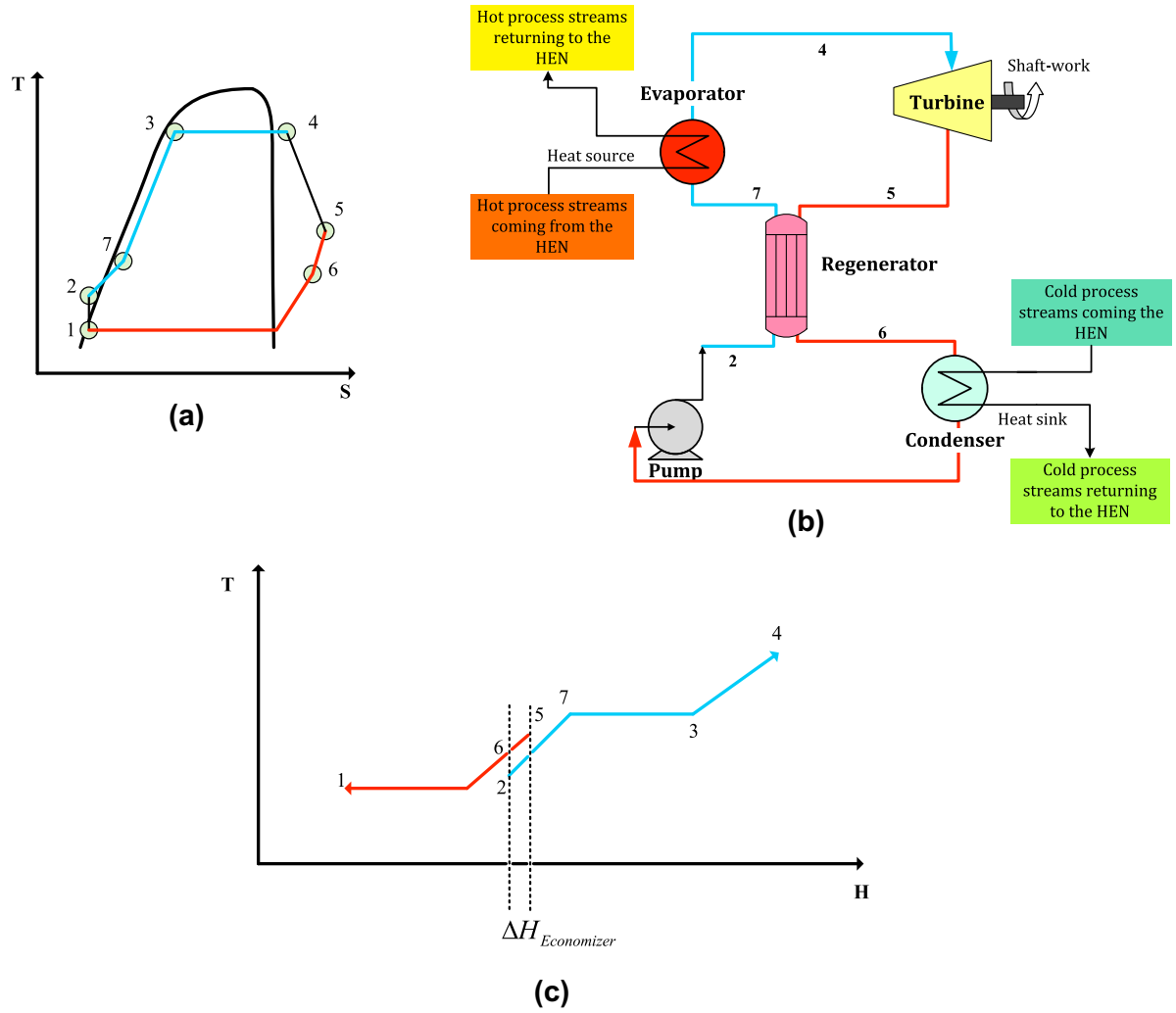

Fig. 2. The regenerative ORC. (a) The cycle on the temperature-entropy diagram. (b) Schematic representation of the cycle integrated with process streams. (c) Heat absorption and heat rejection profiles of the cycle.

stant pressure to state (4). In the fourth process, the saturated vapor expands to state (5) through a turbine to generate power. In the process from state (5) to state (6), the exhaust vapor is utilized in the regenerator to rise the temperature of the sub-cooled liquid entering the evaporator. Finally, in the process from state (6) to state (1), the vapor condenses to state (1) in a water-cooled condenser, thus completing the cycle. Therefore, when the ORC operates alone it absorbs heat from an external low-grade heat source, rejects heat to cooling water, and produces useful shaft-work W or electricity.

The general problem considered in this paper is illustrated in Fig. 2b. The design of the regenerative ORC is not considered as an isolated process; it is integrated with the process streams, therefore heat integration with the process is possible. In this case, the regenerative ORC is allowed to accept heat from hot process streams and to reject heat to cold process streams in order to reduce the overall energy consumption and to produce work. Some of the ORC exhaust heat can be rejected into cooling water. Also, in the integrated system exists heat exchange between hot process streams and cold process streams, in addition to heat transfer between process streams and heating and cooling utilities. Thus, the problem of heat integration within the integrated HEN–ORC system includes matches between many hot streams and cold streams. The hot streams are the hot process streams, the ORC condenser stream, and the hot utility; whereas the cold streams are the cold process streams, the ORC evaporator stream, and the cold utility. Next, to develop a systematic approach for solving the optimization problem of integrated HEN–ORC system, a superstructure is proposed that involves all heat exchange possibilities between hot and cold streams above-mentioned. Fig. 3 is an example superstructure for two hot and two cold process streams representing the heat exchange possibilities within the integrated system. In this representation, the stagewise superstructure for HENs developed by Yee and Grossmann [13] is extended to include an ORC with regenerative working-fluid heating in order to recover the process waste heat for power generation. The ORC uses a dry organic working fluid (i.e., it has a positive slope dS/dT for the saturated vapor line) and consists of heat exchangers (the working fluid cycle's evaporators, condensers and regenerator), the turbine, and the working fluid pump (see Fig. 2).

The integrated superstructure has two major zones: a high-temperature zone in which there is heat exchange between the process streams (i.e., process-to-process heat-exchange zone) and a low-temperature zone that considers the integration of the ORC into the process to generate shaft-work. In addition to these zones, auxiliary cooling and heating are considered at the cold and hot ex-

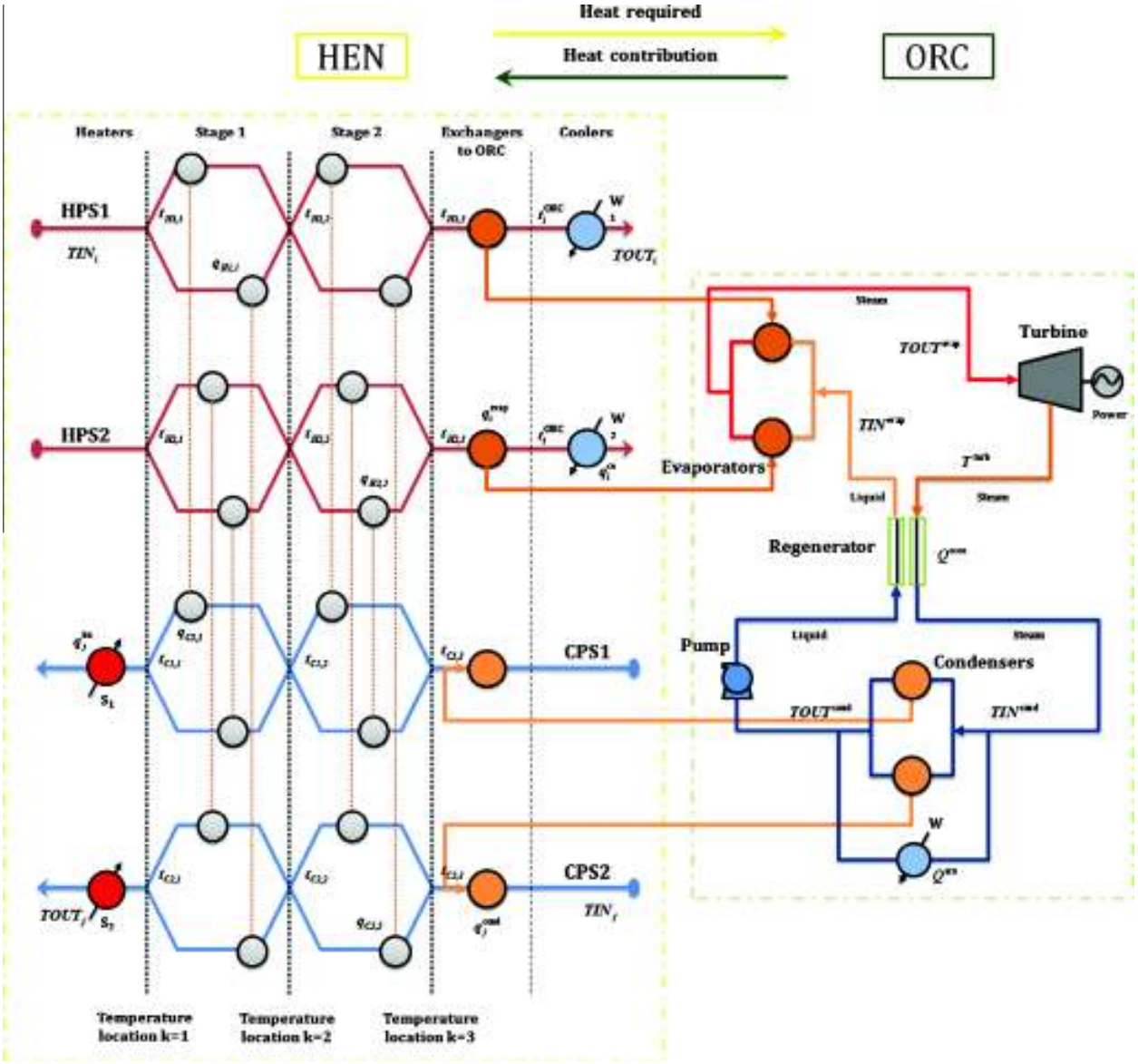

Fig. 3. Superstructure for the integrated HEN–ORC.

tremes of the superstructure, respectively, to satisfy the utility demands. Using the representation in Fig. 3 for the process-to-process heat-exchange zone, and by performing the appropriate material and energy balances at each stage, the corresponding model can be formulated as discussed in Yee and Grossmann [13]. In the integrated zone, low-grade heat from hot process streams is taken to heat the dry organic working fluid in the evaporators, where it is vaporized. The hot process streams and the organic fluid are each confined in separate circulating systems and never come in contact with each other. The saturated vapor is then used to drive the turbine of the ORC for generating shaft work. After leaving the turbine as a superheated vapor, the dry working fluid is employed to raise the temperature of the liquid entering the evaporator. Next, the working fluid rejects its latent heat in the condensers at a lower temperature than the evaporation temperature. As shown in Fig. 3, the heat available from the ORC condensers can be used as the heat needed at low temperature by cold process streams and/or can be rejected into cold utility (i.e., cooling water). Finally, the working fluid condensate is pumped back to the evaporators to complete the cycle.

It should be noted that heat integration between the turbine exhaust gas and cold process streams and/or between the liquid leaving the working fluid pump and hot process streams is not considered for the following reasons. First, dry organic working fluids always yield a dry expansion in the ORC turbine (i.e., the saturated vapor at the turbine's inlet leaves the expander as superheated vapor at state (5) shown in Fig. 2a) which, in turn, causes a significant temperature difference between the superheated vapor exhaust from the turbine and the compressed liquid at the exit of the working fluid pump. The corresponding heat absorption and heat rejection profiles of the cycle are plotted on T–H coordinates in Fig. 2c. Based on these profiles, the following conclusion is obtained: part of the heating requirement (2)–(4) of the ORC can be met by the turbine exhaust (5)–(1). To carry out this internal heat recovery scheme, it is needed a counter-flow heat exchanger (i.e., the ORC regenerator), which raises the temperature

of the sub-cooled liquid leaving the pump by utilizing the turbine exhaust gas. Since the amount of possible heat exchange in the regenerator is very limited as shown in Fig. 2c, it is assumed in this study that the internal heat recovery based on the regenerator has a similar net effect on the integrated system performance that the integration of the regenerator streams with the rest of the process. Second, several works [48–61] have shown that the existence of an economizer (regenerator) to integrate as much as possible the regenerative streams (i.e., thermodynamic processes (5)–(6) and (2)–(7) in Fig. 2a) leads to the best economical solution due to the amount of heat required to be added to the working fluid in the ORC evaporator will be less for a given power output which, in turn, increases the overall efficiency of the cycle. Therefore, it is expected that the regenerator will always appear in the optimal solution if its existence was included in the model as an optimization decision. As a result, it is also assumed in this study that the cycle heat rejection and absorption profiles relevant for the overall integration are given by thermodynamic processes (6)–(1) and (7)–(4) of Fig. 2a, respectively. Finally, if the existence of the regenerator is treated as an optimization variable, the synthesis problem for an integrated HEN–ORC system becomes much more difficult because the corresponding model has to involve nonconvex expressions that limit the possibility to find an optimal solution. Future work would attempt to incorporate the integration of the regenerator streams with the process streams.

The proposed superstructure can easily be generalized to any number of process streams. It should be noted that the temperature levels of stages in the superstructure are considered optimization variables instead of fixed values. Therefore, depending upon the optimal solution, each of the superstructure stages and heat transfer units may exist or not. Also, the model selects the optimal operating conditions (i.e., location in terms of temperature levels) of the stage containing the regenerative ORC integrated with the process streams independently of the magnitude of the temperature differences in the HEN. In this way, it is possible to account simultaneously for the interactions between the heat exchanger networks and ORCs in order to obtain better solutions. Next section presents the formulation of the mathematical programming model associated to the proposed superstructure for any number of process streams.

3. Model formulation

To derive the mathematical model, the following subscripts will be defined to characterize the superstructure. i is used to denote any hot process stream, j is used to denote any cold process stream and k is used to denote any stage in the superstructure. The superscript evap is used to represent an evaporator, cond a condenser, cu the cold utility, hu the hot utility, turb the turbine and econ the regenerator in the ORC. The hot process streams are denoted by the set HPS, and the cold process streams by the set CPS. The set ST represents the stages of the superstructure.

The proposed model is given in the next sub-sections and it includes: overall energy balances for each stream, energy balances for each stage of the superstructure, energy balances for the hot and cold utility, energy balances for evaporators and condensers in the ORC, temperature feasibility constraints, logical relationships to determine the existence of the units required, temperature differences for the heat transfer units when these exist, energy balances for the ORC and the objective function. These equations are stated as follows.

3.1. Overall energy balances for process streams

The total energy balance for each hot process stream i is equal to the sum of the energy exchanged with any cold process stream j at any stage k of the superstructure ($\sum_{k\in ST}\sum_{j\in CPS} q_{i,j,k}$), plus the heat exchanged in the evaporator i located in the ORC (q_i^{evap}) and the heat exchanged with the cold utility i (q_i^{cu}).

$$(TIN_i - TOUT_i)FCp_i = \sum_{k\in ST}\sum_{j\in CPS} q_{i,j,k} + q_i^{evap} + q_i^{cu}, \quad i \in HPS \tag{1}$$

The total energy balance for a cold process stream j is equal to the sum of the heat exchanged with any hot process stream i at any stage k of the superstructure ($\sum_{k\in ST}\sum_{i\in HPS} q_{i,j,k}$), plus the heat exchanged in the condenser j located in the ORC (q_j^{cond}) and the heat supplied by the hot utility j (q_j^{hu}).

$$(TOUT_j - TIN_j)FCp_j = \sum_{k\in ST}\sum_{i\in HPS} q_{i,j,k} + q_j^{cond} + q_j^{hu}, \quad j \in CPS \tag{2}$$

In the above equations *TIN* is the inlet temperature, *TOUT* is the target temperature and *FCp* is the heat capacity flow rate for the process streams.

3.2. Energy balances for matches at each stage of the superstructure

To determine the temperatures for the process streams through the superstructure ($t_{i,k}$, $t_{j,k}$), the next energy balances for each match between hot and cold process streams are used:

$$(t_{i,k} - t_{i,k+1})FCp_i = \sum_{j\in CPS} q_{i,j,k}, \quad k \in ST, \quad i \in HPS \tag{3}$$

$$(t_{j,k} - t_{j,k+1})FCp_j = \sum_{i\in HPS} q_{i,j,k}, \quad k \in ST, \quad j \in CPS \tag{4}$$

3.3. Energy balances for matches between process streams and auxiliary utilities

The requirements of hot and cold utilities (q_j^{hu}, q_i^{cu}) are calculated as follows:

$$(TOUT_j - t_{j,1})FCp_j = q_j^{hu}, \quad j \in CPS \tag{5}$$

$$(t_i^{ORC} - TOUT_i)FCp_i = q_i^{cu}, \quad i \in HPS \tag{6}$$

where $t_{j,1}$ is the temperature of the cold process stream j at stage 1, and t_i^{ORC} is the outlet temperature of the hot process stream i from the exchanger of the ORC. Notice that t_i^{ORC} is lower or equal than the temperature of hot process stream i in the last stage of the superstructure ($t_{i,NOK+1}$). This way, the required cooling utility can be reduced by the use of the excess heat of the hot process streams to run the ORC, reducing simultaneously the associated cost and obtaining economic benefits from the sale of the electric power produced.

3.4. Energy balance for evaporators and condensers in the ORC

The heat loads of the ORC evaporators and condensers are calculated using the temperature of hot and cold process streams, respectively, in the last stage or integrated zone of the superstructure ($t_{i,NOK+1}$, $t_{j,NOK+1}$), so that:

$$(t_{i,NOK+1} - t_i^{ORC})FCp_i = q_i^{evap}, \quad i \in HPS \tag{7}$$

$$(t_{j,NOK+1} - TIN_j)FCp_j = q_j^{cond}, \quad j \in CPS \tag{8}$$

here $t_{j,NOK+1}$ is the temperature of the cold process stream j at the temperature location $NOK + 1$, which is greater or equal than its inlet temperature TIN_j.

3.5. Temperature feasibility constraints

To ensure a monotonic decrement of temperature at each successive stage from left hand side (hottest) to right hand side (coldest) of the superstructure, the following constraints are required:

$$t_{j,NOK+1} \geqslant TIN_j, \quad j \in \text{CPS} \tag{9}$$

$$t_{i,k} \geqslant t_{i,k+1}, \quad k \in \text{ST}, \quad i \in \text{HPS} \tag{10}$$

$$t_{j,k} \geqslant t_{j,k+1}, \quad k \in \text{ST}, \quad j \in \text{CPS} \tag{11}$$

$$TOUT_i \leqslant t_i^{\text{ORC}}, \quad i \in \text{HPS} \tag{12}$$

$$TOUT_j \geqslant t_{j,1}, \quad j \in \text{CPS} \tag{13}$$

Furthermore, the temperature for each hot process stream i at the first stage ($t_{i,1}$) of the superstructure is equal to its inlet temperature:

$$t_{i,1} = TIN_i, \quad i \in \text{HPS} \tag{14}$$

3.6. Logical relationships for the existence of heat transfer units (heat exchangers, coolers, heaters, evaporators and condensers)

The existence of the heat transfer units is modeled using the Big-M formulation [67–70] as follows:

$$q_{i,j,k} - Q_{i,j}^{\max} z_{i,j,k} \leqslant 0, \quad i \in \text{HPS}, \quad j \in \text{CPS}, \quad k \in \text{ST} \tag{15}$$

$$q_i^{\text{cu}} - Q_i^{\max} z_i^{\text{cu}} \leqslant 0, \quad i \in \text{HPS} \tag{16}$$

$$q_j^{\text{hu}} - Q_j^{\max} z_j^{\text{hu}} \leqslant 0, \quad j \in \text{CPS} \tag{17}$$

$$q_i^{\text{evap}} - Q_i^{\max} z_i^{\text{evap}} \leqslant 0, \quad i \in \text{HPS} \tag{18}$$

$$q_j^{\text{cond}} - Q_j^{\max} z_j^{\text{cond}} \leqslant 0, \quad j \in \text{CPS} \tag{19}$$

$$Q^{\text{acu}} - \sum_{i \in \text{HPS}} Q_i^{\max} z^{\text{acu}} \leqslant 0 \tag{20}$$

In previous relationships, $Q^{\max}$ is an upper bound for the heat load in the heat exchangers, coolers, heaters, evaporators and condensers. z is a binary variable used to select the heat transfer units (a value of one indicates that the unit exists and a value of zero indicates that the unit does not exist). Here, if the heat load for a given unit is greater than zero then its corresponding binary variable is equal to one. On the other hand, if the heat load is zero, the corresponding binary variable is set as zero.

3.7. Constraints for the temperature differences in the heat transfer units

When a heat exchanger exists in any stage of the superstructure, the corresponding temperature differences must be calculated properly to satisfy the feasibility constraint for the minimum temperature difference. Therefore, the logical relationships to determine the temperature difference constraints are stated as follows.

For heat exchanger units between process streams:

$$dt_{i,j,k}^{\text{hot}} \leqslant t_{i,k} - t_{j,k} + \Delta T_{ij}^{\max}(1 - z_{i,j,k}), \quad i \in \text{HPS}, \quad j \in \text{CPS}, \quad k \in \text{ST} \tag{21}$$

$$dt_{i,j,k+1}^{\text{cold}} \leqslant t_{i,k+1} - t_{j,k+1} + \Delta T_{ij}^{\max}(1 - z_{i,j,k}), \quad i \in \text{HPS}, \quad j \in \text{CPS}, \quad k \in \text{ST} \tag{22}$$

For coolers:

$$dt_i^{\text{cu-hot}} \leqslant t_i^{\text{ORC}} - TOUT_i^{\text{cu}} + \Delta T_i^{\text{cu-max}}(1 - z_i^{\text{cu}}), \quad i \in \text{HPS} \tag{23}$$

$$dt_i^{\text{cu-cold}} \leqslant TOUT_i - TIN_i^{\text{cu}} + \Delta T_i^{\text{cu-max}}(1 - z_i^{\text{cu}}), \quad i \in \text{HPS} \tag{24}$$

For heaters:

$$dt_j^{\text{hu-hot}} \leqslant TIN_j^{\text{hu}} - TOUT_j + \Delta T_j^{\text{hu-max}}(1 - z_j^{\text{hu}}), \quad j \in \text{CPS} \tag{25}$$

$$dt_j^{\text{hu-cold}} \leqslant TOUT_j^{\text{hu}} - t_{j,1} + \Delta T_j^{\text{hu-max}}(1 - z_j^{\text{hu}}), \quad j \in \text{CPS} \tag{26}$$

For evaporators in the ORC:

$$dt_i^{\text{evap-hot}} \leqslant t_{i,NOK+1} - TOUT^{\text{evap}} + \Delta T^{\text{evap-max}}(1 - z_i^{\text{evap}}), \quad i \in \text{HPS} \tag{27}$$

$$dt_i^{\text{evap-cold}} \leqslant t_i^{\text{ORC}} - TIN^{\text{evap}} + \Delta T^{\text{evap-max}}(1 - z_i^{\text{evap}}), \quad i \in \text{HPS} \tag{28}$$

For condensers in the ORC:

$$dt_j^{\text{cond-hot}} \leqslant TIN^{\text{cond}} - t_{j,NOK+1} + \Delta T^{\text{cond-max}}(1 - z_j^{\text{cond}}), \quad j \in \text{CPS} \tag{29}$$

$$dt_j^{\text{cond-cold}} \leqslant TOUT^{\text{cond}} - TIN_j + \Delta T^{\text{cond-max}}(1 - z_j^{\text{cond}}), \quad j \in \text{CPS} \tag{30}$$

For coolers in the ORC:

$$dt^{\text{acu-hot}} \leqslant TIN^{\text{cond}} - TOUT^{\text{acu}} + \Delta T^{\text{acu-max}}(1 - z^{\text{acu}}) \tag{31}$$

$$dt^{\text{acu-cold}} \leqslant TOUT^{\text{cond}} - TIN^{\text{acu}} + \Delta T^{\text{acu-max}}(1 - z^{\text{acu}}) \tag{32}$$

For regenerator in the ORC:

$$dt^{\text{econ-hot}} \leqslant T^{\text{turb}} - TIN^{\text{evap}} \tag{33}$$

$$dt^{\text{econ-cold}} \leqslant TIN^{\text{cond}} - TOUT^{\text{cond}} \tag{34}$$

In the previous relationships; the binary variable z is used to activate the constraints; therefore, when the heat transfer units exist, the upper limit ($\Delta T^{\max}$) is not considered; whereas when the heat transfer units do not exist the upper limit ($\Delta T^{\max}$) relaxes the relationships.

Finally, to obtain positive heat transfer driving forces, the following constraints must be included:

$$\Delta T^{\min} \leqslant dt_{i,j,k}^{\text{hot}}, \quad i \in \text{HPS}, \quad j \in \text{CPS}, \quad k \in \text{ST} \tag{35}$$

$$\Delta T^{\min} \leqslant dt_{i,j,k+1}^{\text{cold}}, \quad i \in \text{HPS}, \quad j \in \text{CPS}, \quad k \in \text{ST} \tag{36}$$

$$\Delta T^{\min} \leqslant dt_i^{\text{cu-hot}}, \quad i \in \text{HPS} \tag{37}$$

$$\Delta T^{\min} \leqslant dt_i^{\text{cu-cold}}, \quad i \in \text{HPS} \tag{38}$$

$$\Delta T^{\min} \leqslant dt_j^{\text{hu-hot}}, \quad j \in \text{CPS} \tag{39}$$

$$\Delta T^{\min} \leqslant dt_j^{\text{hu-cold}}, \quad j \in \text{CPS} \tag{40}$$

$$\Delta T^{\min} \leqslant dt_i^{\text{evap-hot}}, \quad i \in \text{HPS} \tag{41}$$

$$\Delta T^{\min} \leqslant dt_i^{\text{evap-cold}}, \quad i \in \text{HPS} \tag{42}$$

$$\Delta T^{\min} \leqslant dt_j^{\text{cond-hot}}, \quad j \in \text{CPS} \tag{43}$$

$$\Delta T^{\min} \leqslant dt_j^{\text{cond-cold}}, \quad j \in \text{CPS} \tag{44}$$

$$\Delta T^{\min} \leqslant dt^{\text{acu-hot}} \tag{45}$$

$$\Delta T^{\min} \leqslant dt^{\text{acu-cold}} \tag{46}$$

$$\Delta T^{\min} \leqslant dt^{\text{econ-hot}} \tag{47}$$

$$\Delta T^{\min} \leqslant dt^{\text{econ-cold}} \tag{48}$$

In the above constraints, $\Delta T^{\max}$ and $\Delta T^{\min}$ are upper and lower bounds for the temperature differences at both ends (cold and hot) of the heat transfer units.

3.8. Performance constraints for the regenerative ORC

The performance of the regenerative ORC is evaluated in terms of cycle efficiency defined as the ratio of net shaft-work output to the heat supplied. Hence, the net shaft-work output (E^{ORC}) is given by:

$$E^{\text{ORC}} = \eta^{\text{ORC}} \sum_{i \in \text{HPS}} q_i^{\text{evap}} \tag{49}$$

where η^{ORC} is the ORC efficiency which depends not only on the thermodynamic and thermophysical properties of the chosen working fluid, but also, to a significant extent, on the design configuration and operating conditions of the cycle.

It should be noted that the evaporator saturation temperature (maximum temperature) of the regenerative ORC is determined by the temperature of the available low-grade process heat in the HEN, whereas the condenser saturation temperature (minimum temperature) is set by the temperature of the available cold utility. Desai and Bandyopadhyay [61] showed that for a given value of $\Delta T_{\min}$ the process GCC can be used to select approximately the evaporator temperature at which to operate a regenerative ORC. On the other hand, the condenser temperature is obtained by adding $\Delta T_{\min}$ to the temperature of the cold utility available, so it is fixed implicitly since the temperature level of the cold utility is given in the problem specification. For industrial processes above ambient temperature, cooling water is widely used as a coolant to remove the waste heat; in these cases, the condenser temperature of the regenerative ORC is usually 40 °C, which is just above normal cooling water temperature. Therefore, if detailed thermodynamic data are available for the chosen working fluid, the regenerative ORC efficiency can be calculated prior initiating the optimization process for each specified set of the evaporator and condenser saturation temperatures.

By performing calculations for example problems of regenerative ORCs with fixed temperatures of vaporization and condensation, it has been found that the power consumption of the working fluid pump and the regenerator heat duty are related to the net shaft-work output via a linear function defined through an efficiency parameter (i.e., both increase with increasing cycle shaft-work). Therefore, if the operating temperatures of the cycle remain fixed, the pumping power consumption (E^{pump}) and the regenerator heat duty (Q^{econ}) can be adequately represented by a model of the following form over a range of working fluid flow rates:

$$E^{\text{pump}} = \eta^{\text{pump}} E^{\text{ORC}} \tag{50}$$

$$Q^{\text{econ}} = \eta^{\text{econ}} E^{\text{ORC}} \tag{51}$$

where η^{pump}, η^{econ} are the efficiency parameters associated with the working fluid pump and the ORC regenerator, respectively. It should be noted that the efficiency parameters can be calculated prior to integration of the ORC. η^{pump} usually takes values lower than 0.06 [48] and η^{econ} lower than 0.045 [48].

The total heat load (Q^{total}) of the condensers can now be determined by performing an overall energy balance for the regenerative ORC represented by the following equation:

$$Q^{\text{total}} = \sum_{i \in \text{HPS}} q_i^{\text{evap}} + E^{\text{pump}} - E^{\text{ORC}} \tag{52}$$

In addition, the total heat available at low temperature from the condensers of the ORC can be sent to heat the cold process streams j ($\sum_{j \in \text{CPS}} q_j^{\text{cond}}$) and/or can be rejected into the cold utility (Q^{acu}) as follows:

$$Q^{\text{total}} = \sum_{j \in \text{CPS}} q_j^{\text{cond}} + Q^{\text{acu}} \tag{53}$$

3.9. Objective function

The objective function consists in minimizing the total annual cost (*TAC*), which is the sum of the operating cost (*Cop*) and the annualized capital cost (*Cap*), minus the revenue from the sale of the electricity that is generated by the ORC (*Sprc*).

$$\min TAC = Cop + Cap - Sprc \tag{54}$$

The operating cost includes the costs due to the cold and hot utility requirements and to the power (electricity) needed to operate the working fluid pump,

$$Cop = \text{H}_Y \sum_{i \in \text{HPS}} \text{C}^{\text{cu}} q_i^{\text{cu}} + \text{H}_Y \sum_{j \in \text{CPS}} \text{C}^{\text{hu}} q_j^{\text{hu}} + \text{H}_Y \text{C}^{\text{acu}} Q^{\text{acu}} + \text{H}_Y \text{C}^{\text{pump}} E^{\text{pump}} \tag{55}$$

where H_Y is the annual operating time, C^{cu} is the unitary cost of the cold utility required for the hot process stream i, C^{hu} is the unitary cost of the hot utility required for the cold process stream j, C^{acu} is the unitary cost for the cold utility required in the ORC, C^{pump} is the unitary cost of the power demanded by the pump required in the ORC and E^{pump} is the power consumption of the working fluid pump. The capital cost depends on the type, number, and size of units utilized to satisfy the design objectives. A substantial part of the operating cost usually depends upon the utilities consumed.

The annualized capital cost involves the fixed charges (*Capf*) and variable (*Capv*) capital costs for heat transfer units (including the heat exchangers between process streams, coolers, heaters, evaporators and condensers) as well as for the pump, turbine and regenerator installed in the ORC,

$$Cap = Capf + Cap\,v \tag{56}$$

The fixed-charge costs (*Capf*) are independent of the size of the units and are expressed as follows:

$$Capf = K_F \sum_{i \in \text{HPS}} \sum_{j \in \text{CPS}} \sum_{k \in \text{ST}} \text{CF} z_{i,j,k} + \text{K}_F \sum_{i \in \text{HPS}} \text{CF}^{\text{cu}} z_i^{\text{cu}} + \text{K}_F \sum_{j \in \text{CPS}} \text{CF}^{\text{hu}} z_j^{\text{hu}} + \text{K}_F \sum_{i \in \text{HPS}} \text{CF}^{\text{evap}} z_i^{\text{evap}} + \text{K}_F \sum_{j \in \text{CPS}} \text{CF}^{\text{cond}} z_j^{\text{cond}} + \text{K}_F \text{CF}^{\text{acu}} z^{\text{acu}} + \text{K}_F \text{CF}^{\text{econ}} + \text{K}_F \text{CF}^{\text{turb}} + \text{K}_F \text{CF}^{\text{pump}} \tag{57}$$

The variable capital costs (*Capv*) depend on the size of the units according to the following equation:

$$
\begin{aligned}
Capv = {} & K_F \sum_{i\in HPS}\sum_{j\in CPS}\sum_{k\in ST} CV\left\{\frac{q_{i,j,k}(1/h_i+1/h_j)}{[(dt_{i,j,k}^{hot})(dt_{i,j,k+1}^{cold})(dt_{i,j,k}^{hot}+dt_{i,j,k+1}^{cold})/2+\delta]^{1/3}}\right\}^{\beta^{exch}} \\
& + K_F \sum_{i\in HPS} CV^{cu}\left\{\frac{q_i^{cu}(1/h_i+1/h^{cu})}{[(dt_i^{cu\text{-}hot})(dt_i^{cu\text{-}cold})(dt_i^{cu\text{-}hot}+dt_i^{cu\text{-}cold})/2+\delta]^{1/3}}\right\}^{\beta^{cu}} \\
& + K_F \sum_{j\in CPS} CV^{hu}\left\{\frac{q_j^{hu}(1/h^{hu}+1/h_j)}{[(dt_j^{hu\text{-}hot})(dt_j^{hu\text{-}cold})(dt_j^{hu\text{-}hot}+dt_j^{hu\text{-}cold})/2+\delta]^{1/3}}\right\}^{\beta^{hu}} \\
& + K_F \sum_{i\in HPS} CV^{evap}\left\{\frac{q_i^{evap}(1/h_i+1/h^{evap})}{[(dt_i^{evap\text{-}hot})(dt_i^{evap\text{-}cold})(dt_i^{evap\text{-}hot}+dt_i^{evap\text{-}cold})/2+\delta]^{1/3}}\right\}^{\beta^{evap}} \\
& + K_F \sum_{j\in CPS} CV^{cond}\left\{\frac{q_j^{cond}(1/h^{cond}+1/h_j)}{[(dt_j^{cond\text{-}hot})(dt_j^{cond\text{-}cold})(dt_j^{cond\text{-}hot}+dt_j^{cond\text{-}cold})/2+\delta]^{1/3}}\right\}^{\beta^{cond}} \\
& + K_F CV^{acu}\left\{\frac{Q^{acu}(1/h^{cond}+1/h^{acu})}{[(dt^{acu\text{-}hot})(dt^{acu\text{-}cold})(dt^{acu\text{-}hot}+dt^{acu\text{-}cold})/2+\delta]^{1/3}}\right\}^{\beta^{cu}} \\
& + K_F CV^{econ}\left\{\frac{Q^{econ}(1/h^{econ\text{-}hot}+1/h^{econ\text{-}cold})}{[(dt^{econ\text{-}hot})(dt^{econ\text{-}cold})(dt^{econ\text{-}hot}+dt^{econ\text{-}cold})/2+\delta]}\right\}^{\beta^{econ}} \\
& + K_F CV^{turb}\left\{E^{ORC}\right\}^{\beta^{turb}} + K_F CV^{pump}\left\{E^{pump}\right\}^{\beta^{pump}}
\end{aligned}
\tag{58}
$$

where K_F is a factor used to annualize the inversion to take into account the interest rate and the value of the money in the time through the life of the project, β is a parameter used to consider the economies of scale (it usually takes a value between 0.6 and 0.8), CF is the unitary fixed capital cost for the process units considered, CV is the unitary variable capital cost for the units considered, Q^{econ} is the heat load in the regenerator located in the ORC, δ is a small parameter (i.e. 1×10^{-6}) used to avoid division by zero in the objective function. To calculate the variable capital costs of the heat transfer units, the heat transfer areas are considered and these are calculated using the Chen's approximation [71] to estimate the mean-logarithmic temperature differences.

Finally, the revenue from the sale of the generated electricity in the ORC is calculated as follows:

$$Sprc = H_Y C^{power} E^{ORC} \tag{59}$$

where C^{power} is the unitary selling price for the electricity and E^{ORC} is the generated power in the ORC.

The proposed model was coded in the software GAMS [72] and the solvers CPLEX, CONOPT and DICOPT were used for solving the associated linear, non-linear and mixed-integer non-linear programming problems, respectively.

4. Results

To show the application of the proposed model, three examples were solved. The data are given in Table 1, which includes the data for hot and cold process streams, for external hot and cold utilities, as well as for the operating temperatures of the major components of the ORC (condenser, evaporator, turbine and economizer or regenerator). In addition, the values for the parameters K_F, H_Y, ΔT^{min}, β, C, *COP*, CF and CV are presented in the Table 2. R245fa, *n*-pentane and *n*-hexane (dry fluids) are used as working fluids for Examples 1–3, respectively, because these organic fluids provide good efficiencies for ORCs [59–61]. To show the advantages of the application of the integrated HEN–ORC system, the addressed problems were solved with and without the integration of the ORC. Examples 2 and 3 were originally proposed by Desai and Bandyopadhyay [61] for illustrating their sequential integration approach, whose solution is compared with the simultaneous integration proposed in the present paper.

Table 1
Data for examples.

Stream/unit	TIN (°C)	TOUT (°C)	FCP (kW/°C)	h (kW/m^2 °C)
Example 1				
HPS1	300	80	30	1
HPS2	200	40	45	1
CU	10	40		1
CPS1	40	180	40	1
CPS2	140	280	60	1
HU	350	220		1
Evaporator	40	100		1
Condenser	40	30		1
CU–ORC	10	20		1
Regenerator				0.5
Turbine		50.7		
Example 2				
HPS1	187	77	300	1
HPS2	127	27	500	1
CU	15	30		1
CPS1	147	217	600	1
CPS2	47	117	200	1
HU	300	250		1
Evaporator	40.2	87.5		1
Condenser	60.1	40		1
CU–ORC	15	30		1
Regenerator				0.5
Turbine		70		
Example 3				
HPS1	353	313	9.802	1
HPS2	347	246	2.931	1
HPS3	255	80	6.161	1
CU	15	30		1
CPS1	224	340	7.179	1
CPS2	116	303	0.641	1
CPS3	53	113	7.627	1
CPS4	40	293	1.690	1
HU	460	370		1
Evaporator	81	186.5		1
Condenser	135.9	80		1
CU–ORC	15	30		1
Regenerator				0.5
Turbine		161		

Table 2
Economic parameters for examples.

Example	1	2	3
K_F (year^{-1})	0.23	0.23	0.23
H_Y (h/year)	8000	8000	8000
ΔT^{min} (°C)	20	10	20
β (dimensionless)	0.65	0.65	0.65
C^{hu} (US$/kW year)	192.096	192.096	192.096
C^{cu} (US$/kW year)	10.1952	10.1952	10.1952
C^{pump} (US$/kW h)	0.07	0.07	0.07
C^{power} (US$/kW h)	0.07	0.07	0.07
COP^{ORC}	0.144	0.139	0.144
COP^{pump}	0.0204	0.0204	0.0204
COP^{econ}	0.0124	0.0124	0.0124
CF	0	0	0
CV	1650	1650	1650

Example 1. This example, taken from Ahmad et al. [7], consists of two hot and two cold process streams, along with one hot and one cold utility. The operating temperatures and efficiency parameters for the ORC, which operates between maximum and minimum temperature limits of 100 °C and 30 °C, respectively, were taken from Saleh et al. [62]. The synthesis problem was solved first without considering the heat integration of the ORC with the process streams (this case is labeled as the Scenario A). The resulting optimal configuration is shown in Fig. 4. The HEN requires three heat transfer units between process streams, one cooler for the hot process stream HPS1 and one for HPS2, and a

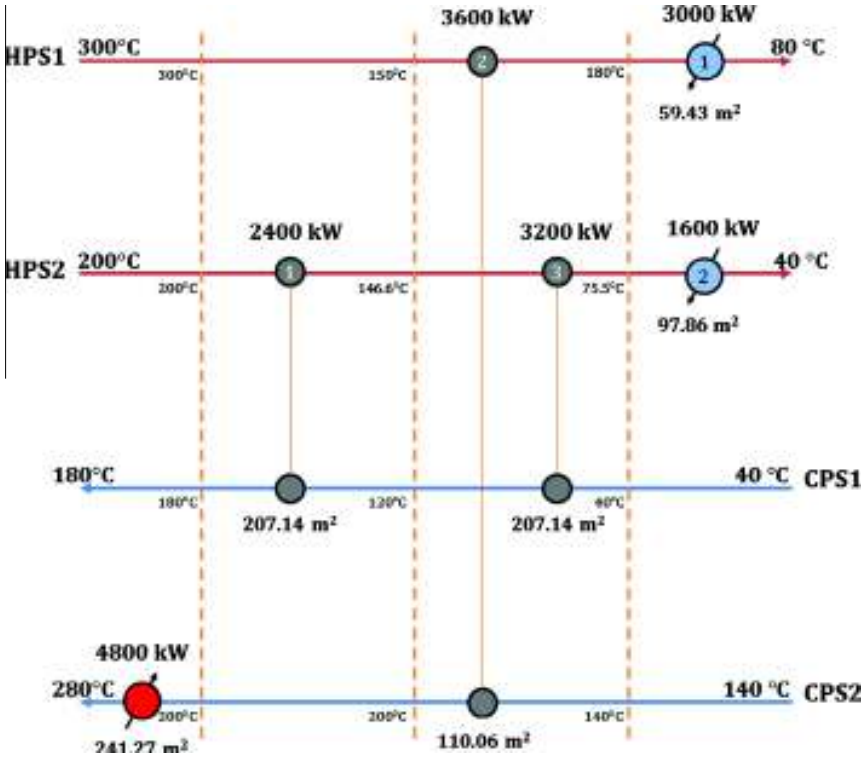

Fig. 4. Optimal HEN for Example 1 without integrating the ORC (Scenario A).

heater for the cold process stream CPS2. As can be seen in Table 3, the area of the network is 923 m^2, for a total capital cost of US$45,818/year and a total annual cost of US$1,014,776/year. The utility requirements are 4800 kW of steam and 4600 kW of cooling water. Notice in Table 3 that the optimal network shows hot utility cost equals to 90.8% of the total annual cost, whereas the cold utility cost and capital costs represent 4.6% and 4.5% of the *TAC*, respectively. Hence the utility cost is very significant respect to the total annual cost for this example.

The optimal solution obtained by the proposed method for the integrated system (labeled as the Scenario B) is shown in Fig. 5. It requires a total area of 1332 m^2 and eight heat transfer units (three heat exchangers, one heater, one cooler, one evaporator, one condenser, and the regenerator), with a total capital cost of US$86,437/year and a total annual cost of US$1,056,161/year. The utility demands for the integrated system are 10.86 kW of electricity to drive the working fluid pump in the ORC, 3178.06 kW of cooling water for the ORC condenser, 4800 kW of steam for the HEN heater, and 900 kW of cooling water for the HEN cooler. Notice that 532.8 kW of electricity are generated by the ORC. Also notice that the ORC condenser is not integrated with the process, so the only heat integration that takes place between the HEN and the ORC is in the evaporator of the ORC (i.e. a heat exchange match between the hot process stream HPS2 and the working fluid). Only 3700 kW of the total amount of low-grade heat available (4600 kW in stream HPS2) for power generation are absorbed by the ORC evaporator.

As can be observed in Fig. 5, the optimal heating requirement for the integrated system is identical to the one obtained in Fig. 4 for Scenario A. But the integrated system reduces the overall cold utility consumption of the individual network by 11.6% (532.8 kW), from 4600 kW to 4067.2 kW. As the integrated system is in overall energy balance, this saving in cold utility is accompanied by an identical quantity of shaft-work produced by the ORC. This implies that the waste heat load reduction (i.e., reduction in the overall cold utility requirement due to integration of the ORC and the process) is transformed into shaft-work on a one to one basis (i.e., 100% first law efficiency of work generation).

Table 3
Comparison of results for Example 1.

Concept	HEN – Scenario A	HEN–ORC – Scenario B
Total heat transfer area (m^2)	923	1332
Total waste heat reused (kW)	0	3700
Total power produced (kW)	–	532
Capital costs		
Heat exchangers (US$/year)	22,231	20,087
Heaters (US$/year)	13,423	13,423
Coolers (US$/year)	10,164	22,226
Evaporators (US$/year)	–	13,698
Regenerator (US$/year)	–	698
Turbine (US$/year)	–	15,930
Pump (US$/year)	–	375
Operating costs		
Heating (US$/year)	922,060	922,060
Cooling (US$/year)	46,897	41,577
Pumping (US$/year	–	6087
Total capital cost (US$/year)	45,818	86,437
Total operating cost (US$/year)	968,959	969,724
Total income from electricity sales (US$/year)	–	298,368
Total annual cost (US$/year)	1,014,776	757,794

The comparison of Figs. 5 and 4 shows that the integration of the ORC into the overall process introduces two additional heat transfer units (8 for Scenario B vs. 6 for Scenario A). It also in-

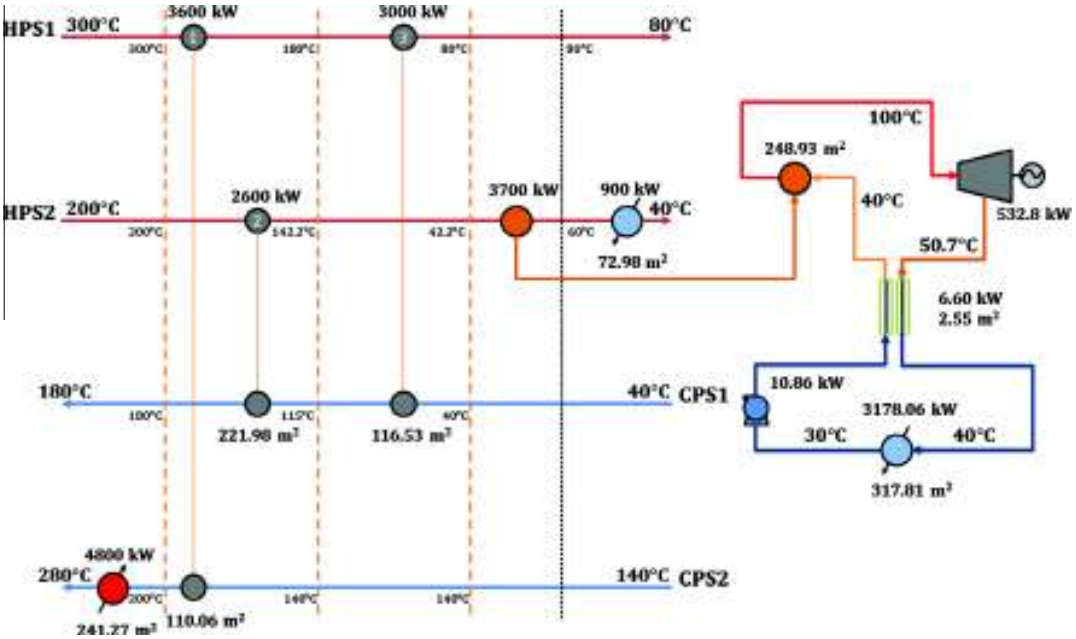

Fig. 5. Optimal integrated HEN–ORC for Example 1 (Scenario B).

creases the total heat transfer area required and hence the capital cost. Notice in Table 3 that the integrated system (Scenario B) has a total area and a total capital cost that are 44.3% and 88.65% higher than those for the individual network (Scenario A). However, it is interesting to note that this marked difference in the capital cost is not very important since Scenario A and Scenario B show total operating costs equal to 95.5% and 91.82%, respectively, of the sum of the corresponding total operating cost and total capital cost. As consequence, the operating costs are the major costs for this example. Also, notice that the integrated system has an annual revenue of 298,368 US$/year due to the sale of electricity generated by the ORC. That explains why the total annual cost for the individual network is 33.9% higher than that of the integrated system (1,014,776 US$/year vs. 757,794 US$/year).

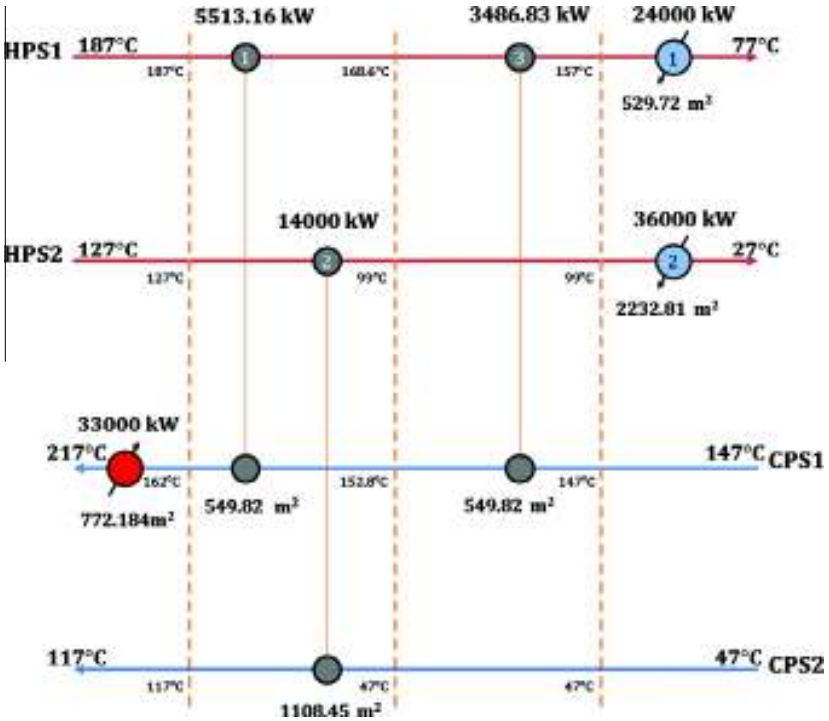

Fig. 6. HEN without the integration of the ORC for Example 2 (Scenario A).

Table 4
Results for Example 2.

Concept	HEN – Scenario A	HEN–ORC [61] – Scenario B	HEN–ORC – Scenario C
Total heat transfer area (m^2)	5743	10,714	11,231
Total waste heat reused (kW)	0	36,936	48,400
Total power produced (kW)	–	5134	6728
Capital costs			
Heat exchangers (US$/year)	56,601	102,045	46,874
Heaters (US$/year)	28,591	28,590	28,592
Coolers (US$/year)	65,473	119,757	113,252
Evaporators (US$/year)	–	60,619	86,965
Regenerator (US$/year)	–	1614	2065.00
Turbine (US$/year)	–	153,510	201,155
Pump (US$/year)	–	7227	4735
Operating costs			
Heating (US$/year)	6,339,168	6,339,168	6,339,168
Cooling (US$/year)	611,712	578,149	544,522
Pumping (US$/year	–	117,304	76,856
Total capital cost (US$/year)	150,665	473,362	483,637
Total operating cost (US$/year)	6,950,880	7,034,621	6,960,546
Total income from electricity sales (US$/year)	–	2,875,098	3,767,456
Total annual cost (US$/year)	7,101,545	4,632,885	3,676,727

Example 2. The second example consists of determining the optimum integrated system for two hot streams, two cold streams, one hot utility, and one cold utility. The minimum temperature difference is specified as 10 °C. This example was taken from Desai and Bandyopadhyay [61] for showing the advantages of the simultaneously approach here proposed with respect to the sequential approach implemented by Desai and Bandyopadhyay [61]. Therefore, the optimal integrated HEN–ORC obtained with the proposed approach (Scenario C) is compared with the configuration reported by Desai and Bandyopadhyay [61] (Scenario B), and also with the optimal HEN without considering the ORC (Scenario A).

The optimum design for Scenario A is shown in Fig. 6 and consists of six units (three heat exchangers, two coolers, and one heater) with a total area of 5743 m^2. The hot utility required is 33,000 kW and the cold utility is 60,000 kW. The process-to-process heat recovery is 23,000 kW. This configuration has a total annual cost of US$7,101,545/year formed by 98% of operating cost and 2% of capital cost, whose values are disaggregated in Table 4.

The sequential solution obtained by Desai and Bandyopadhyay [61] is presented in Fig. 7; where there are two heat exchangers between process streams (HPS1–CPS1 and HPS2–CPS2), two coolers and one heater, as well as two evaporators, one condenser and one regenerator. The heating utility is 33,000 kW of steam and the cooling utility is 56,708 kW of cooling water. In the ORC evaporators, the working fluid takes heat from process streams HPS1 and HPS2 to produce 5134.1 kW of shaft power. Table 4 shows the results of Fig. 7. It is important to note that the capital cost of Fig. 7 was calculated here because it was not considered by Desai and Bandyopadhyay [61]. Notice in Table 4 that the integrated solution of Scenario B respect to Scenario A increases the total capital and operational costs by 68% and 1%, respectively; however, the shaft work produced in Scenario B represents savings by 62% in the total cost yielding a solution with a net *TAC* 35% lower than the solution of Scenario A.

Fig. 8 presents the optimal configuration (Scenario C) for the integrated HEN–ORC obtained with the simultaneous approach proposed in this paper. Notice in Fig. 8 that there are two heat exchangers between process streams (HPS1–CPS1 and HPS1–CPS2), and that the ORC takes 48,400 kW of low-grade heat both from the hot process streams HPS1 and HPS2. Here the produced electricity is 6728 kW. As Example 1, only the ORC evaporator is integrated with the process due to the condenser rejects all its heat into cold utility. As shown in Table 4, this solution features a minimum total annual cost of US$7,444,183/year, from which 93.5% corresponds to the operating cost (external utilities) and 6.5% to the capital cost. Notice that the shaft power produced by the

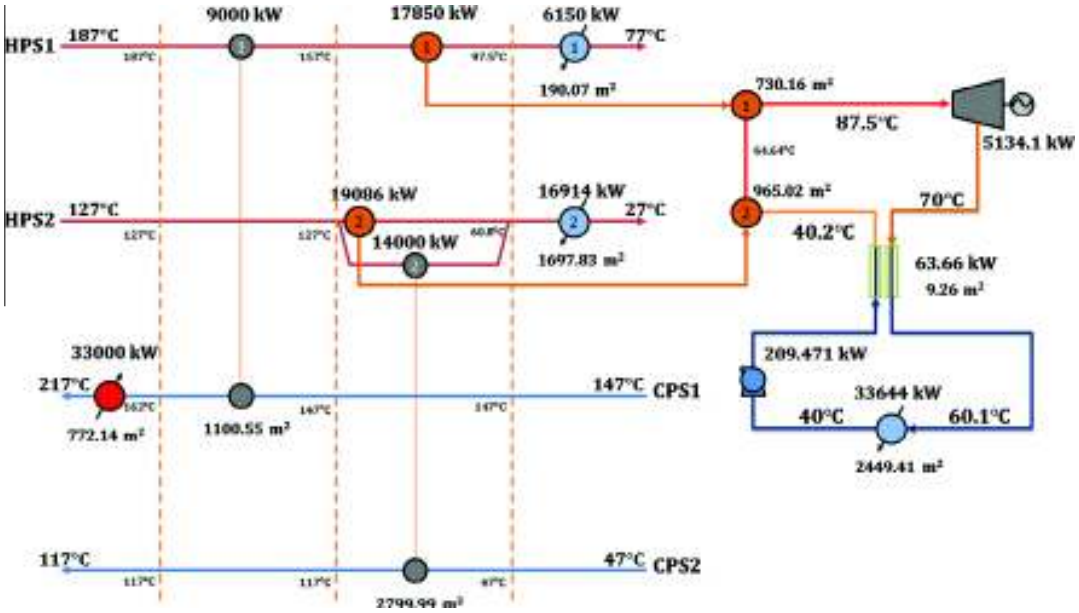

Fig. 7. Sequential HEN–ORC configuration for Example 2 (Scenario B [61]).

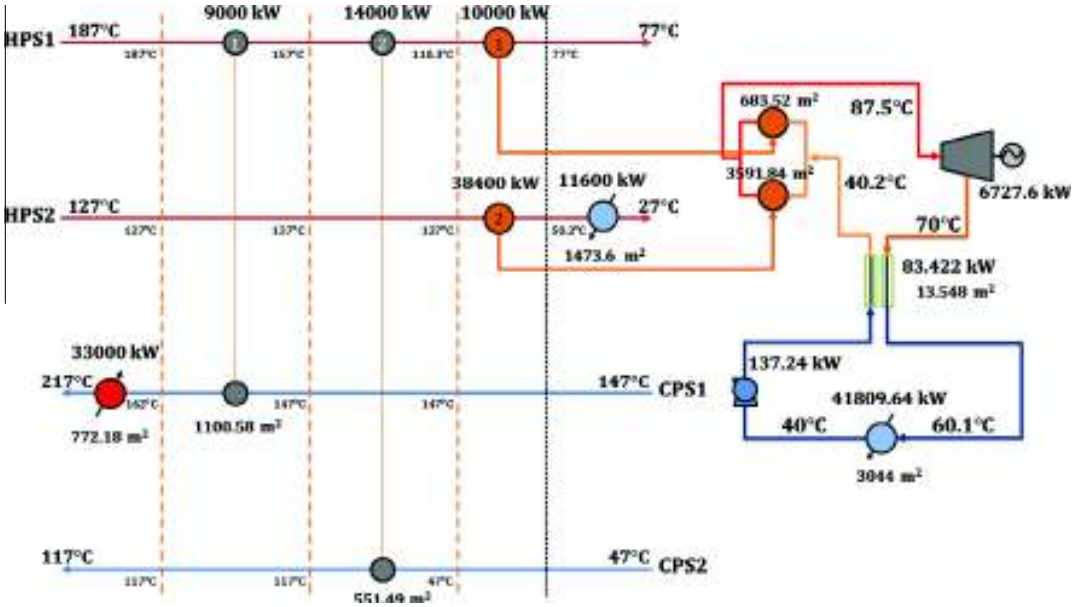

Fig. 8. Optimal integrated HEN–ORC for Example 2 using the simultaneous approach proposed in this paper (Scenario C).

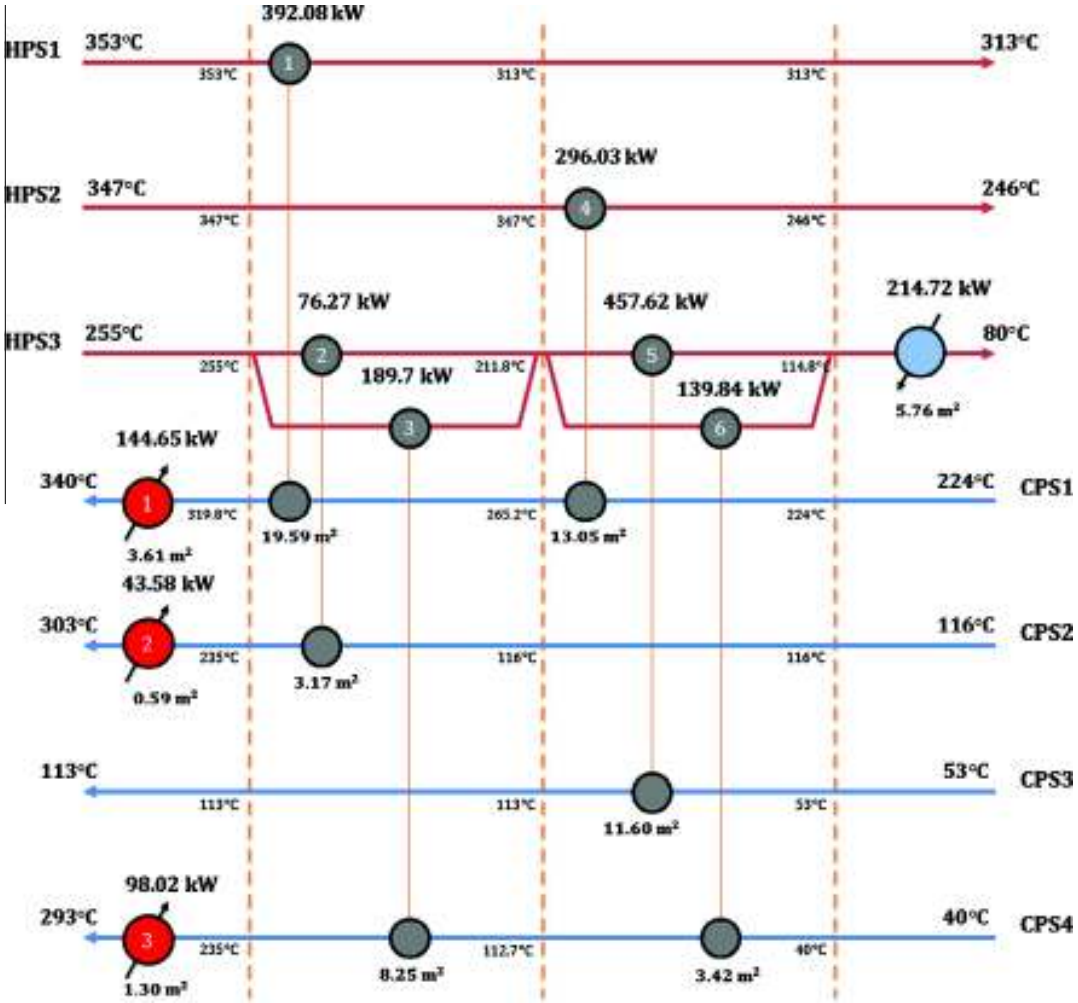

Fig. 9. Optimal HEN without considering the ORC for Example 3 (Scenario A).

ORC yields annual savings ofUS$3,767,456/year, which yields savings by 49% in the net *TAC* (i.e., US$3,676,727/year).

The results for the three scenarios are shown in Table 4, so it can be used to make a comparison of the optimal solution (Scenario C) obtained from the proposed MINLP model with the solutions for Scenario A and Scenario B. First, the capital cost obtained for the solution of Scenario C is US$483,637/year, which represents an increase of 2.1% and 221% in the capital cost with respect to the solutions for Scenarios B and A, respectively. It is important to note, however, that the capital cost is insignificant respect to the cost of utilities in this particular example. On the other hand, also notice that the integrated system for Scenario C produces 6728 kW of electricity, which is 31% higher than that of Scenario B, whereas there is not production of electricity in Scenario A. Clearly, the main feature of the results in Table 4 is that with the sequential procedure (Scenario B) the *TAC* is 26% higher than with the proposed simultaneous procedure for obtaining the solution of Scenario C (US$4,632,885/year vs. US$3,676,727/year). The main reason for this difference is that the proposed procedure yields an integrated system with higher production of shaft power (6728 kW vs. 5134 kW). This difference in *TAC* is due to the sequential method focuses only on the minimum utility consumption as design objective when synthesizing the integrated system, whereas the proposed MINLP model can properly take into account the economic trade-offs between capital and energy including the shaft power produced by the ORC.

Example 3. This example is also taken from Desai and Bandyopadhyay [61] and involves three hot streams, three cold streams, one hot utility, and one cold utility. For this example, the minimum temperature difference is 20 °C. The ORC cycle absorbs heat at 90°C and rejects it at 30°C. The optimal configuration and operating conditions for the individual network (Scenario A) are shown in Fig. 9. Notice that in this configuration there are six heat exchangers between process streams, one cooler for the hot process stream HPS3 and three heaters (for the cold process streams CPS1, CPS2 and CPS4). Here the total heat transfer area is 70 m^2 and the external cooling and heating requirements are 214.7 kW and 286.3 kW, respectively. Desai and Bandyopadhyay [61] reported the optimal integrated system for this problem shown in Fig. 10 (Scenario B). The number of heat transfer units of this solution is 18 (ten heat exchangers, two heaters, four condensers, one evaporator, and one regenerator), which is significantly greater than the one for Scenario A, but it produces 48.62 kW of shaft power. In this case, the process stream HPS3 transfers 337.7 kW of heat to the ORC, and also process streams CPS3 and CPS4 receive thermal energy from the condensers of the ORC (165.2 kW). The integrated system for Scenario B requires a total heat transfer area of 128 m^2. On the other hand, the optimal configuration (Scenario C) of the integrated system generated by solving the proposed MINLP formulation is shown in Fig. 11. This design has thirteen heat transfer units (seven heat exchangers, one cooler for the hot process stream HPS3, one heater for the cold process stream CPS1, one evaporator, two condensers, and one regenerator). The ORC evaporator takes its heat (682.11 kW) from the hot process stream HPS3. In this design, the ORC condensers reject heat into the process (457.62 kW and 128.27 kW for cold streams CPS3 and CPS4, respectively), so it is also integrated with the process. The total heat transfer area for this Scenario C is 153 m^2 and the produced electricity is 98 kW.

Table 5 shows the main results for the three different scenarios presented for Example 3. Notice in Table 5 that the total heat transfer areas for Scenarios A and B represent reductions by 54% and 16% respect to Scenario C, respectively. The operational costs for Scenarios A and B represent reductions by 3.9% and 17.13% respect to Scenario C, respectively; whereas the capital costs for Scenario A

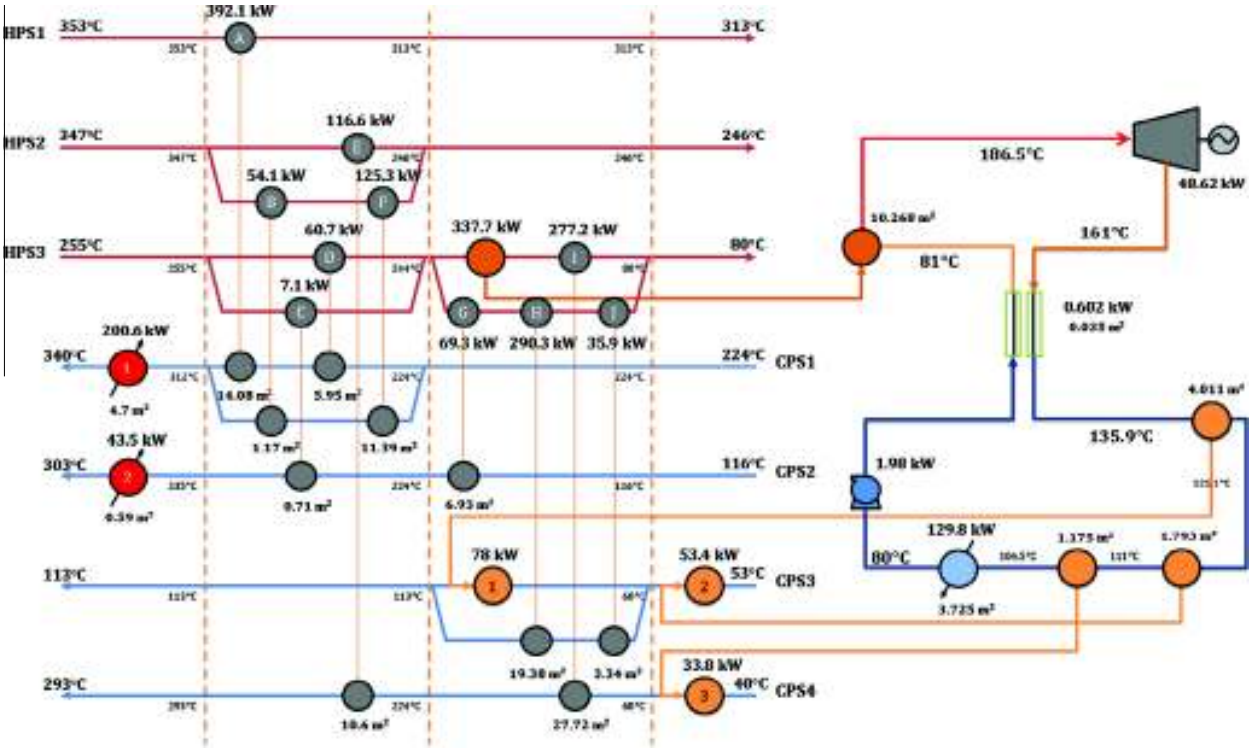

Fig. 10. HEN–ORC for Example 3 using the sequential approach (Scenario B [61]).

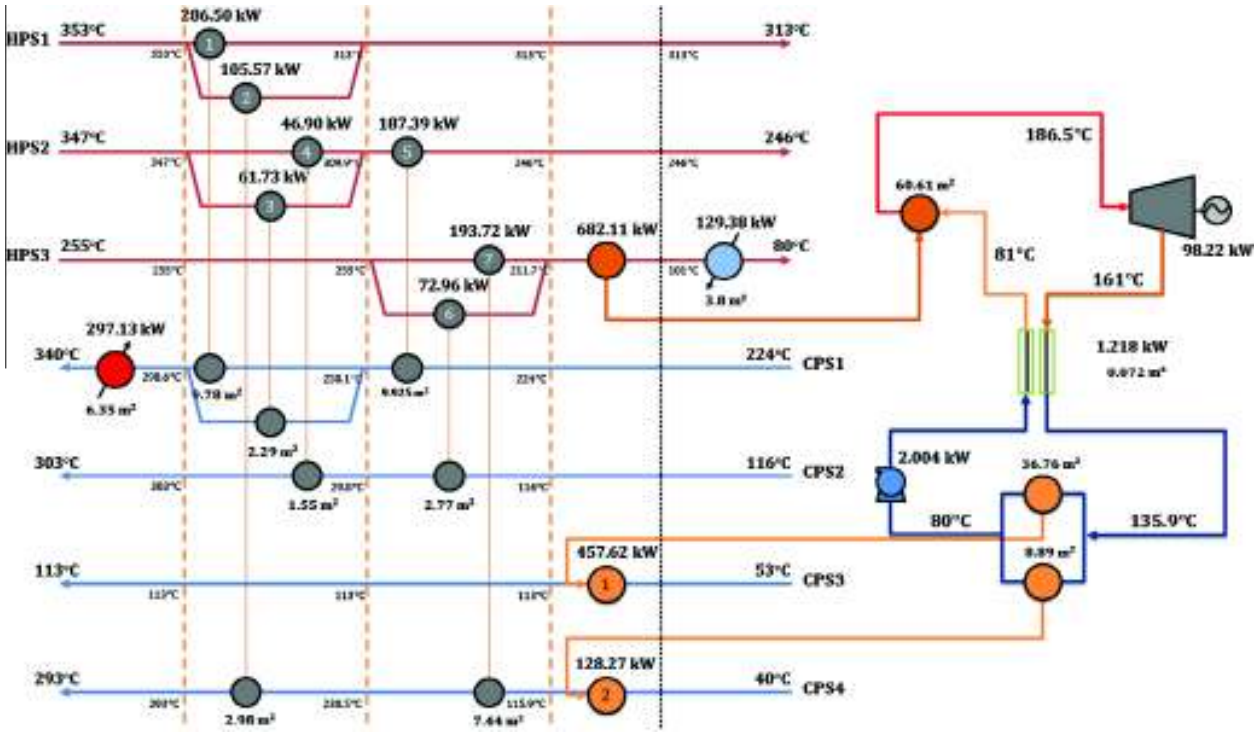

Fig. 11. Optimal simultaneously integrated HEN–ORC for Example 3 (Scenario C).

Table 5
Results for Example 3.

Concept	HEN – Scenario A	HEN–ORC [61] – Scenario B	HEN–ORC – Scenario C
Total heat transfer area (m^2)	70	128	153
Total waste heat reused (kW)	0	337.7	682.11
Total power produced (kW)	–	49	98
Capital costs			
Heat exchangers (US$/year)	5380	15,722	3952
Heaters (US$/year)	1152	1310	1262
Coolers (US$/year)	1185	892	905
Evaporators (US$/year)	–	1725	5469
Condensers (US$/year)		1912	4549
Regenerator (US$/year)	–	44	69
Turbine (US$/year)	–	1454	2937
Pump (US$/year)	–	68	70
Operating costs			
Heating (US$/year)	54,990	46,891	57,079
Cooling (US$/year)	2189	1323	1319
Pumping (US$/year	–	1111	1122
Total capital cost (US$/year)	7717	23,127	19,212
Total operating cost (US$/year)	57,179	49,325	59,520
Total income from electricity sales (US$/year)	–	27,232	55,005
Total annual cost (US$/year)	64,896	45,220	23,726

is 59.83% lower than the one of Scenario C and the capital costs for Scenario B is 17% greater than the one of Scenario C. This way, the total cost (operating and capital) for Scenarios A and B are 17.57% and 8% lower than the one corresponding to Scenario C. However, the energy produced in Scenario B is 50.49% lower than the one of Scenario C and the shaft work produced in Scenario A is zero. These solutions yield net total annual costs of US$64,896/year, US$45,220/year and US$23,726/year for Scenarios A–C, respectively. Notice that the net *TAC* of the solutions of Scenarios A and B are 173.52% and 90.59% greater than the solution of Scenario C. Thus, proposed MINLP formulation provides an optimal configuration for the integrated system that is a better solution that the one that can be obtained from the sequential approach, because of a better trade-off between the energy and capital costs.

Previous examples have shown that the use of the simultaneous optimization holistic approach for designing integrated HEN–ORC

Table 6
Problem size and CPU time for each example presented.

Concept	Example 1		Example 2		Example 3	
	Scenario B	Scenario A	Scenario C	Scenario A	Scenario C	Scenario A
Constraints	96	69	96	69	191	150
Continuous variables	90	61	90	61	190	146
Binary variables	17	12	17	12	39	31
CPU time (s)	0.030	0.025	0.030	0.030	0.032	0.046

systems allows reducing significantly the associated costs in the energy integration process.

Finally, Table 6 shows the size for each problem addressed in this paper as well as the CPU time consumed in a computer with an i5-2430 M processor at 2.4 GHz and 4 GB of RAM.

5. Conclusions

In this paper, a procedure based on mixed integer nonlinear programming is proposed for the simultaneous optimization of processes involving integrated heat recovery and power generation based on ORCs. The proposed method simultaneously optimizes the configuration and operational parameters of the integrated system considering the capital and operational costs as well as the sale of the electric power produced, minimizing this way the net total annual cost of the integrated process. The proposed optimization can be easily solved in a short CPU time.

Three examples problems were used to illustrate the application of the proposed approach. Results show that when optimizing this kind of process energy systems, important savings can be obtained when the process and the ORC are optimized simultaneously to achieve a high degree of heat integration. In particular, the effectiveness of the proposed method was illustrated by finding improved solutions for two previously published case studies (Examples 2 and 3) that were solved using a sequential approach. Also, the solution of the examples showed that when stand-alone heat exchangers networks are only synthesized, a higher *TAC* is always obtained. In the context of overall processes, the results obtained suggest that the problem of selecting an ORC for recovering low-grade process excess heat in power generation must be addressed simultaneously with the problem of determining the optimum heat exchanger network.

The proposed MINLP formulation is general and can be applied to any case study with the corresponding data.

Acknowledgments

The authors acknowledge the financial support from the Mexican Council of Science and Technology (CONACYT) and the Scientific Research Council of the Universidad Michoacana de San Nicolás de Hidalgo.

References

[1] Gundersen T, Naess L. The synthesis of cost optimal heat exchanger networks an industrial review of the state of the art. Comput Chem Eng 1988;12(6):503–30.
[2] Jezowski J. Heat exchanger network grassroots and retrofit design. The review of the state-of-the-art: Part I. Heat-exchanger network targeting and insight based methods of synthesis. Hung J Ind Chem 1994;22(4):279–94.
[3] Jezowski J. Heat exchanger network grassroots and retrofit design. The review of the state-of-the-art: Part II. Heat-exchanger network synthesis by mathematical-methods and approaches for retrofit design. Hung J Ind Chem 1994;22(4):295–308.
[4] Furman KC, Sahinidis NV. A critical review and annotated bibliography for heat exchanger network synthesis in the 20th century. Ind Eng Chem Res 2002;41(10):2335–70.
[5] Linnhoff B, Hindmarsh E. The pinch design method for heat exchanger networks. Chem Eng Sci 1983;38(5):745–63.
[6] Ahmad S. Cost optimum heat exchanger networks minimum energy and capital using simple models for capital costs. Comput Chem Eng 1990;14(7):729–50.
[7] Ahmad S, Linnhoff B, Smith R. Cost optimum heat exchanger networks-2. Targets and design for detailed capital cost models. Comput Chem Eng 1990;14(7):751–67.
[8] Cerda JA, Westerberg W, Mason D, Linnhoff B. Minimum utility usage in heat exchanger network synthesis a transportation problem. Chem Eng Sci 1983;38(3):373–87.
[9] Colberg RD, Morari M. Area and capital cost targets for heat exchanger network synthesis with constrained matches and unequal heat transfer coefficients. Comput Chem Eng 1990;14(1):1–22.
[10] Floudas CA, Ciric AR, Grossmann IE. Automatic synthesis of optimum heat exchanger network configurations. Am Inst Chem Engrs 1986;32(2):276–90.
[11] Papoulias SA, Grossmann IE. A structural optimization approach in process synthesis-I: utility systems. Comput Chem Eng 1983;7(6):695–706.
[12] Ciric AR, Floudas CA. Heat exchanger network synthesis without decomposition. Comput Chem Eng 1991;15(6):385–96.
[13] Yee TF, Grossmann IE. Simultaneous optimization models for heat integration-II. Heat exchanger network synthesis. Comput Chem Eng 1990;14(10):1165–84.
[14] Ponce-Ortega JM, Jimenez-Gutierrez A, Grossmann IE. Simultaneous retrofit and heat integration of chemical processes. Ind Eng Chem Res 2008;47(15):5512–28.
[15] Linnhoff B, Townsend DW, Boland D, Hewitt GF, Thomas BEA, Buy AR, et al. User guide on process integration for the efficient use of energy. Rugby, UK: The Institution of Chemical Engineers; 1982.
[16] Costa ALH, Queiroz EM. An extension of the problem table algorithm for multiple utilities targeting. Energy Convers Manage 2009;50(4):1124–8.
[17] Salama AIA. Optimal assignment of multiple utilities in heat exchange networks. Appl Therm Eng 2009;29(13):2633–42.
[18] Viswanathan M, Evans LB. Studies in the heat integration of chemical process plants. Am Inst Chem Engrs 1987;33(11):1781–90.
[19] Serna-González M, Jiménez-Gutiérrez A, Ponce-Ortega JM. Targets for heat exchanger network synthesis with different heat transfer coefficients and non-uniform exchanger specifications. Chem Eng Res Des 2007;85(10):1447–57.
[20] Serna-González M, Ponce-Ortega JM. Total cost target for heat exchanger networks considering simultaneously pumping power and area effects. Appl Therm Eng 2011;31(11–12):1964–75.
[21] Castier M. Rigorous multiple utility targeting in heat exchanger networks. Energy Convers Manage 2012;59:74–85.
[22] Smith R, Jobson M, Chen L. Recent development in the retrofit of heat exchanger networks. Appl Therm Eng 2010;30(16):2281–9.
[23] Wang Y, Pan M, Bulatov I, Smith R, Kim JK. Application of intensified heat transfer for the retrofit of heat exchanger network. Appl Energy 2012;89(1):45–59.
[24] Wang Y, Smith R, Kim JK. Heat exchanger network retrofit optimization involving heat transfer enhancement. Appl Therm Eng 2012;43:7–13.
[25] Verheyen W, Zhang N. Design of flexible heat exchanger network for multi-period operation. Chem Eng Sci 2006;61(23):7730–53.
[26] Chen L, Hung PS. Simultaneous synthesis of flexible heat-exchange networks with uncertain source-stream temperatures and flow rates. Ind Eng Chem Res 2004;43(18):5916–28.
[27] Konukman AES, Camurdan MC, Akman U. Simultaneous flexibility targeting and synthesis of minimum-utility heat-exchanger networks with superstructure-based MILP formulation. Chem Eng Process 2002;41(6):501–18.
[28] Serna-González M, Ponce-Ortega JM, Jiménez-Gutiérrez A. Two-level optimization algorithm for heat exchanger networks including pressure drop considerations. Ind Eng Chem Res 2004;43(21):6766–73.
[29] Mizutani FT, Pessoa FLP, Queiroz EM, Hauan S, Grossmann IE. Mathematical programming model for heat-exchanger network synthesis including detailed heat exchanger designs. 2. Network synthesis. Ind Eng Chem Res 2003;42(17):4019–27.
[30] Frausto-Hernández S, Rico-Ramírez V, Jiménez-Gutiérrez A, Hernández-Castro S. MINLP synthesis of heat exchanger networks considering pressure drop effects. Comput Chem Eng 2003;27:1143–52.
[31] Ponce-Ortega JM, Serna-González M, Jiménez-Gutiérrez A. Heat exchanger networks synthesis including detailed heat exchanger design using genetic algorithms. Ind Eng Chem Res 2007;46(25):8767–80.
[32] Ponce-Ortega JM, Serna-González M, Jiménez-Gutiérrez A. Synthesis of multipass heat exchanger networks using genetic algorithms. Comput Chem Eng 2008;32(10):2320–32.

[33] Sorsak A, Kravanja Z. MINLP retrofit of heat exchanger networks comprising different exchanger types. Comput Chem Eng 2004;28(1–2):235–51.
[34] Ma KL, Hui CW, Yee TF. Constant approach temperature model for HEN retrofit. Appl Therm Eng 2000;20(15–16):1505–33.
[35] Ponce-Ortega JM, Jiménez-Gutiérrez A, Grossmann IE. Optimal synthesis of heat exchanger networks involving isothermal process streams. Comput Chem Eng 2008;32(8):1918–42.
[36] Hasan MMF, Karimi IA, Alfadala HE, Grootjans H. Operational modeling of multistream heat exchangers with phase changes. Am Inst Chem Engrs 2009;55(1):150–71.
[37] Kamath RS, Biegler LT, Grossmann IE. Modeling multi-stream heat exchangers with and without phase changes for simultaneous optimization and heat integration. Am Inst Chem Engrs 2012;58(1):190–204.
[38] Ponce-Ortega JM, Serna-González M, Jiménez-Gutiérrez A. Synthesis of heat exchanger networks with optimal placement of multiple utilities. Ind Eng Chem Res 2010;49(6):2849–56.
[39] López-Maldonado LA, Ponce-Ortega JM, Segovia-Hernández JG. Multiobjective synthesis of heat exchanger networks minimizing the total annual cost and the environmental impact. Appl Therm Eng 2011;31(6–7):1099–113.
[40] Ponce-Ortega JM, Serna-González M, Jiménez-Gutiérrez A. MINLP synthesis of optimal cooling networks. Chem Eng Sci 2007;62(21):5728–35.
[41] Ponce-Ortega JM, Serna-González M, Jiménez-Gutiérrez A. A disjunctive programming model for simultaneous synthesis and detailed design of cooling networks. Ind Eng Chem Res 2009;48(6):2991–3003.
[42] Ponce-Ortega JM, Serna-González M, Jiménez-Gutiérrez A. Optimization model for re-circulating cooling water systems. Comput Chem Eng 2010;34(2):177–95.
[43] Rubio-Castro E, Serna-González M, Ponce-Ortega JM. Optimal design of effluent-cooling systems using a mathematical programming model. Appl Therm Eng 2010;30(14–15):2116–26.
[44] Rubio-Castro E, Serna-González M, Ponce-Ortega JM, El-Halwagi MM. Synthesis of cooling water systems with multiple cooling towers. Appl Therm Eng 2013;50(1):957–74.
[45] Lira-Barragán LF, Ponce-Ortega JM, Serna-González M, El-Halwagi MM. Synthesis of integrated absorption refrigeration systems involving economic and environmental objectives and quantifying social benefits. Appl Therm Eng 2013;52(2):402–19.
[46] Ponce-Ortega JM, Tora EA, González-Campos JB, El-Halwagi MM. Integration of renewable energy with industrial absorption refrigeration systems: systematic design and operation with technical, economic, and environmental objectives. Ind Eng Chem Res 2011;50(16):9667–84.
[47] Wechsung A, Aspelund A, Gundersen T, Barton PI. Synthesis of heat exchanger networks at subambient conditions with compression and expansion of process streams. Am Inst Chem Engrs 2011;57(8):2090–108.
[48] Lee KM, Kuo SF, Chien ML, Shih YS. Parameters analysis on organic Rankine cycle energy recovery system. Energy Convers Manage 1988;28(2):129–36.
[49] Hung TC, Shai TY, Wang SK. A review of organic Rankine cycles (ORCs) for the recovery of low-grade waste heat. Energy 1997;22(7):661–7.
[50] Hung TC. Waste heat recovery of organic Rankine cycle using dry fluids. Energy Convers Manage 2001;42(5):539–53.
[51] Hettiarachchi MHD, Golubovic M, Worek WM, Ikegami Y. Optimum design criteria for an organic Rankine cycle using low-temperature geothermal heat sources. Energy 2007;32(9):1698–706.
[52] Dai Y, Wang J, Gao L. Parametric optimization and comparative study of organic Rankine cycle (ORC) for low grade waste heat recovery. Energy Convers Manage 2009;50(3):576–82.
[53] Schuster A, Karellas S, Kakaras E, Spliethoff H. Energetic and economic investigation of organic Rankine cycle applications. Appl Therm Eng 2009;29(8–9):1809–17.
[54] Roy JP, Mishra MK, Misra A. Parametric optimization and performance analysis of a waste heat recovery system using organic Rankine cycle. Energy 2010;35(12):5049–62.
[55] Wang H, Peterson R, Herron T. Design study of configurations on system COP for a combined ORC (organic Rankine cycle) and VCC (vapor compression cycle). Energy 2011;36(8):4809–20.
[56] Quoilin S, Declaye S, Tchanche B, Lemort V. Thermo-economic optimization of waste heat recovery organic Rankine cycles. Appl Therm Eng 2011;31(14):2885–93.
[57] Mago PJ, Luck R. Energetic and exergetic analysis of waste heat recovery from a microturbine using organic Rankine cycles. Int J Energy Res 2012.
[58] Zhang J, Zhang W, Hou G, Fang F. Dynamic modeling and multivariable control of organic Rankine cycles in waste heat utilizing processes. Comput Math Appl 2012;64(5):908–21.
[59] Papadopoulos AI, Stijepovic M, Linke P. On the systematic design and selection of optimal working fluids for organic Rankine cycles. Appl Therm Eng 2010; 30(6–7):760–9.
[60] Wang ZQ, Zhou NJ, Guo J, Wang XY. Fluid selection and parametric optimization of organic Rankine cycle using low temperature waste heat. Energy 2012;40(1):107–15.
[61] Desai NB, Bandyopadhyay S. Process integration of organic Rankine cycle. Energy 2009;34(10):1674–86.
[62] Saleh B, Koglbauer G, Wendland M, Fischer J. Working fluids for low-temperature organic Rankine cycles. Energy 2007;32(7):1210–21.
[63] Cheng WL, Chen ZS, Hu P, Jia L. A new generalized four-parameter corresponding states method for predicting volumetric behavior of working fluids. Int J Thermophys 2001;22(6):1769–79.
[64] Liu BT, Chien KH, Wang CC. Effect of working fluids on organic Rankine cycle for waste heat recovery. Energy 2004;29(8):1207–17.
[65] Wang EH, Zhang HG, Fan BY, Ouyang MG, Zhao Y, Mu QH. Study of working fluid selection of organic Rankine cycle (ORC) for engine waste heat recovery. Energy 2011;36(5):3406–18.
[66] Stijepovic M, Linke P, Papadopoulos AI, Grujic A. On the role of working fluid properties in organic Rankine cycle performance. Appl Therm Eng 2012; 36:406–13.
[67] Raman R, Grossmann IE. Modelling and computational techniques for logic based integer programming. Comput Chem Eng 1994;18(7):563–78.
[68] Lee S, Grossmann IE. New alghorithms for nonlinear generalized disjuntive programming. Comput Chem Eng 2000;24(9–10):2125–41.
[69] Vecchietti A, Lee S, Grossmann IE. Modeling of discrete/continuous optimization problems: characterization and reformulation of disjunctions and their relaxations. Comput Chem Eng 2003;27(3):443–8.
[70] Ruiz JP, Grossmann IE. A hierarchy of relaxations for nonlinear convex generalized disjunctive programming. Eur J Oper Res 2012;218:38–47.
[71] Chen JJJ. Comments on improvement on a replacement for the logarithmic mean. Chem Eng Sci 1987;42(10):2488–9.
[72] Brooke, Kendrick D, Meeraus A, Raman R. GAMS user's guide. USA: The Scientific Press; 2013.